

**Unusually High Fluorescence Quantum Yield of a Homopolyfluorenylazomethine -  
Towards A Universal Fluorophore**

Charlotte Mallet,<sup>†</sup> Andréanne Bolduc,<sup>†</sup> Sophie Bishop,<sup>†</sup> Yohan Gautier,<sup>†</sup> and W.G. Skene\*

Laboratoire de caractérisation photophysique des matériaux conjugués  
Département de Chimie, Pavillon JA Bombardier,  
Université de Montréal, CP 6128, succ. Centre-ville,  
Montréal, Québec, Canada H3C 3J7

<sup>†</sup>Authors contributed equally

**Electronic Supplementary Information (ESI)**

Electronic Supplementary Information (ESI) Available: Complete material characterization data.

## Table of Contents

Figure S1. Normalized absorbance spectra of <b>1</b> in toluene (■), ether (●), tetrahydrofuran (▲), ethyl acetate (▼), chloroform (▶), dichloromethane (◀), acetonitrile (◆), and ethanol (◇). .....	6
Figure S2. Lippert-Mataga plot showing the Stokes shift of <b>1</b> as a function of the solvent orientation polarizability ( $\Delta f$ ). .....	6
Figure S3. Uncorrected fluorescence of <b>1</b> as a function of $E_T(30)$ in various solvents. ....	7
Figure S4. Uncorrected fluorescence quenching of <b>1</b> as a function of nitrobenzene concentration from 0 (—) to 1 (—) mM. ....	7
Figure S5. Stern-Volmer quenching of <b>1</b> as a function of nitrobenzene. ....	8
Figure S6. Uncorrected fluorescence quenching of <b>1</b> as a function of 2,6-dinitrotoluene concentration from 0 (—) to 2.2 (—) mM. ....	8
Figure S7. Stern-Volmer quenching of <b>1</b> as a function of 2,6-dinitrotoluene. ....	9
Figure S8. Uncorrected fluorescence quenching of <b>1</b> as a function of nitromethane concentration from 0 (—) to 250 (—) mM. ....	9
Figure S9. Stern-Volmer quenching of <b>1</b> as a function of nitromethane. ....	10
Figure S10. Temperature dependent uncorrected fluorescence of <b>1</b> in ethanol/methanol (4:1) at 300 K (◆) and 77 K (◇). ....	10
Figure S11. Temperature dependent uncorrected fluorescence of <b>1</b> in methylcyclohexane at 300 K (■) and 77 K (□). ....	11
Figure S12. Temperature dependent uncorrected fluorescence of <b>1</b> in ether/pentane/EtOH (5:5:1) at 300 K (▶) and 77 K (▷). ....	11
Figure S13. Relative corrected fluorescence of <b>1</b> in dichloromethane without (—) and with trifluoroacetic acid (—) added. ....	12
Figure S14. Corrected fluorescence of <b>1</b> in dichloromethane (—), chloroform (—), methylcyclohexane (—) excited at 345 nm with matching absorbance at 345 nm measured with identical instrument parameters. ....	12
Table S1. Fluorescence lifetimes of <b>1</b> measured in various solvents. <sup>a</sup> .....	13
Figure S15. Fluorescence kinetics of <b>1</b> monitored at 427 nm in dichloromethane. ....	13
Figure S16. Fluorescence kinetics of <b>1</b> monitored at 427 nm in dichloromethane (yellow), instrument response frequency (blue), biexponential numerical fit (pink) taking into account the instrument response frequency, and residual fitting between measured and fitting data (green). .	14
Figure S17. Fluorescence kinetics of <b>1</b> monitored at 405 nm in tetrahydrofuran. ....	14
Figure S18. Fluorescence kinetics of <b>1</b> monitored at 405 nm in tetrahydrofuran (yellow), instrument response frequency (blue), biexponential numerical fit (pink) taking into account the instrument response frequency, and residual fitting between measured and fitting data (green). .	15
Figure S19. Fluorescence kinetics of <b>1</b> monitored at 463 nm in methylcyclohexane. ....	15
Figure S20. Fluorescence kinetics of <b>1</b> monitored at 463 nm in methylcyclohexane (yellow), instrument response frequency (blue), triexponential numerical fit (pink) taking into account the instrument response frequency, and residual fitting between measured and fitting data (green). .	16
Figure S21. Fluorescence kinetics of <b>1</b> monitored at 430 nm in acetonitrile. ....	16
Figure S22. Fluorescence kinetics of monitored <b>1</b> at 430 nm in acetonitrile (yellow), instrument response frequency (blue), triexponential numerical fit (pink) taking into account the instrument response frequency, and residual fitting between measured and fitting data (green). ....	17
Figure S23. Fluorescence kinetics of <b>1</b> monitored at 390 nm in toluene. ....	17

Figure S24. Fluorescence kinetics of <b>1</b> monitored at 390 nm in toluene (yellow), instrument response frequency (blue), triexponential numerical fit (pink) taking into account the instrument response frequency, and residual fitting between measured and fitting data (green). .....	18
Figure S25. Fluorescence kinetics of <b>1</b> monitored at 475 nm in ethanol. ....	18
Figure S26. Fluorescence kinetics of <b>1</b> monitored at 475 nm in ethanol (yellow), instrument response frequency (blue), monoexponential numerical fit (pink) taking into account the instrument response frequency, and residual fitting between measured and fitting data (green), truncated from 6 to 33 ns.....	19
Figure S27. Fluorescence kinetics of <b>1</b> monitored at 475 nm in ethanol (yellow), instrument response frequency (blue), monoexponential numerical fit (pink) taking into account the instrument response frequency, and residual fitting between measured and fitting data (green). .	19
Figure S28. Normalized absorbance spectra of <b>2</b> in toluene (■), ether (●), tetrahydrofuran (▲), ethyl acetate (▼), chloroform (►), dichloromethane (◄), acetonitrile (●), and ethanol (◆). ....	20
Figure S29. Lippert-Mataga plot showing the Stokes shift of <b>2</b> as a function of solvent orientation polarizability ( $\Delta f$ ). .....	20
Figure S30. Fluorescence of <b>2</b> as a function of $E_T(30)$ in various solvents. ....	21
Figure S31. Uncorrected fluorescence quenching of <b>2</b> as a function of nitrobenzene concentration from 0 (—) to 2.7 (—) mM. ....	21
Figure S32. Stern-Volmer quenching of <b>2</b> as a function of nitrobenzene. ....	22
Figure S33. Stern-Volmer quenching of <b>2</b> as a function of 2,6-dinitrotoluene. ....	22
Figure S34. Uncorrected fluorescence quenching of <b>2</b> as a function of nitromethane concentration from 0 (—) to 160 (—) mM. ....	23
Figure S35. Stern-Volmer quenching of <b>2</b> as a function of nitromethane. ....	23
Figure S36. Temperature dependent uncorrected fluorescence of <b>2</b> in dichloromethane between 300 K (—) and 190 K (—). ....	24
Figure S37. Temperature dependent uncorrected fluorescence of <b>2</b> in ethanol/methanol (4:1) at 300 K (◆) and 77 K (◇). ....	24
Figure S38. Temperature dependent uncorrected fluorescence of <b>2</b> in methylcyclohexane at 300 K (■) and 77 K (□). ....	25
Figure S39. Temperature dependent uncorrected fluorescence of <b>2</b> in ether/pentane/EtOH (5:5:1) at 300 K (►) and 77 K (▷). ....	25
Figure S40. Normalized absorbance (●) and uncorrected fluorescence (○) spectra of <b>2</b> deposited as a thin film on a glass substrate. ....	26
Figure S41. Normalized absorbance (►) and uncorrected fluorescence (▷) spectra of <b>2</b> in a thin film PMMA matrix deposited as a thin film on a glass substrate. ....	26
Table S2. Fluorescence lifetimes of <b>2</b> measured in various solvents. <sup>a</sup> .....	27
Figure S42. Fluorescence kinetics of <b>2</b> monitored at 491 nm in ethanol: methanol (4:1). ....	27
Figure S43. Fluorescence kinetics of <b>2</b> monitored at 489 nm in dichloromethane. ....	28
Figure S44. Fluorescence kinetics of <b>2</b> monitored at 489 nm in dichloromethane (yellow), instrument response frequency (blue), biexponential numerical fit (pink) taking into account the instrument response frequency, and residual fitting between measured and fitting data (green). .	28
Figure S45. Fluorescence kinetics of <b>2</b> monitored at 466 nm in ethyl acetate. ....	29
Figure S46. Fluorescence kinetics of <b>2</b> monitored at 466 nm in ethyl acetate (yellow), instrument response frequency (blue), biexponential numerical fit (pink) taking into account the instrument response frequency, and residual fitting between measured and fitting data (green). ....	29
Figure S47. Fluorescence kinetics of <b>2</b> monitored at 440 nm in methylcyclohexane. ....	30

Figure S48. Fluorescence kinetics of <b>2</b> monitored at 440 nm in methylcyclohexane (yellow), instrument response frequency (blue), triexponential numerical fit (pink) taking into account the instrument response frequency, and residual fitting between measured and fitting data (green).	30
Figure S49. Fluorescence kinetics of <b>2</b> monitored at 467 nm in tetrahydrofuran.	31
Figure S50. Fluorescence kinetics of <b>2</b> monitored at 467 nm in tetrahydrofuran (yellow), instrument response frequency (blue), biexponential numerical fit (pink) taking into account the instrument response frequency, and residual fitting between measured and fitting data (green).	31
Figure S51. Fluorescence kinetics of <b>2</b> monitored at 546 nm in ethanol.	32
Figure S52. Fluorescence kinetics of <b>2</b> monitored at 546 nm in ethanol (yellow), instrument response frequency (blue), biexponential numerical fit (pink) taking into account the instrument response frequency, and residual fitting between measured and fitting data (green).	32
Figure S53. Fluorescence kinetics of <b>2</b> monitored at 491 nm in dichloromethane (—), methylcyclohexane (—), and ethanol: methanol (4:1) (—).	33
Figure S54. Uncorrected fluorescence spectra of <b>3</b> ( $M_n=7200$ g/mol) measured in various solvents: toluene (black), dichloromethane (red), acetonitrile (blue), ether (green), THF (pink), ethyl acetate (olive), chloroform (navy), and ethanol (wine).	33
Figure S55. Uncorrected fluorescence spectra of quinine bisulfate in 0.5 M sulfuric acid (black) and <b>3</b> (red) magnified 100 times in dichloromethane excited at 370 nm.	34
Figure S56. Polarisation fluorescence spectra of <b>2</b> measured in dichloromethane.	34
Figure S57. Fluorescence spectra in nitrogen (solid line) and oxygen purged (dashed line) solvents: <b>1</b> in dichloromethane (—) and ethanol (—) and <b>2</b> in dichloromethane (—) and ethanol (—).	35
Figure S58. Transient absorbance emission kinetics of <b>2</b> monitored at 500 nm with a photomultiplier tube in anhydrous and deaerated dichloromethane after exciting at 423 nm. Fluorescence lifetime is $6.07 \pm 0.07$ ns.	35
Figure S59. Transient absorbance spectrum of <b>2</b> measured in anhydrous and deaerated dichloromethane 0 (■), 800 (○), 1600 (▲), 2400 (▽) and 3200 (◆) ns after exciting at 423 nm. Inset: transient absorbance kinetics of <b>2</b> monitored at 500 nm in anhydrous and deaerated dichloromethane after exciting at 423 nm.	36
Figure S60. Transient absorbance emission kinetics of <b>2</b> monitored at 500 nm with a photomultiplier tube in deaerated tetrahydrofuran after exciting at 423 nm. Fluorescence lifetime is $5.81 \pm 0.07$ ns.	36
Figure S61. Transient absorbance spectrum of <b>2</b> in anhydrous and deaerated tetrahydrofuran 0 (■), 4 (○), 8 (▲), 12 (▽) and 16 (◆) ns after exciting at 423 nm. Inset: transient absorbance kinetics of <b>2</b> monitored at 500 nm in anhydrous and deaerated dichloromethane after exciting at 423 nm.	37
Figure S62. Transient absorbance emission kinetics of <b>2</b> monitored at 500 nm with a photomultiplier tube in anhydrous and deaerated toluene after exciting at 423 nm. Fluorescence lifetime is $5.9 \pm 0.2$ ns.	37
Figure S63. Transient absorbance spectrum of <b>2</b> in anhydrous and deaerated toluene after 0 (■), 800 (○), 1600 (▲), 2400 (▽) and 3200 (◆) ns after exciting at 423 nm. Inset: transient absorbance kinetics of <b>2</b> monitored at 500 nm in anhydrous and deaerated dichloromethane after exciting at 423 nm.	38
Figure S64. Corrected emission spectra of <b>3</b> in toluene at room temperature (red) and 77 K (black) excited at 285 nm.	38

Figure S65. Corrected emission spectra of <b>3</b> in 2-methyl-tetrahydrofuran at room temperature (red) and 77 K (black) excited at 285 nm.....	39
Figure S66. Anodic cyclic voltammograms of <b>1</b> (red) and <b>2</b> (black) in dichloromethane with Bu <sub>4</sub> NPF <sub>6</sub> measured with a scan speed of 200 mV/sec. Ferrocene was added to <b>2</b> as an internal reference.....	39
Scheme S1. Synthetic scheme for the preparation of <b>3</b> and its corresponding monomers. ....	40
Synthesis.....	40
Figure S67. <sup>1</sup> H NMR of <b>5</b> in acetone-d <sub>6</sub> .....	43
Figure S68. <sup>1</sup> H NMR <b>8</b> in acetone-d <sub>6</sub> .....	44
Figure S69. <sup>1</sup> H NMR of <b>3</b> in CDCl <sub>3</sub> after 84 h of polymerization. ....	45
Figure S70. GPC elugram of <b>3</b> in THF relative to polystyrene standards. ....	46

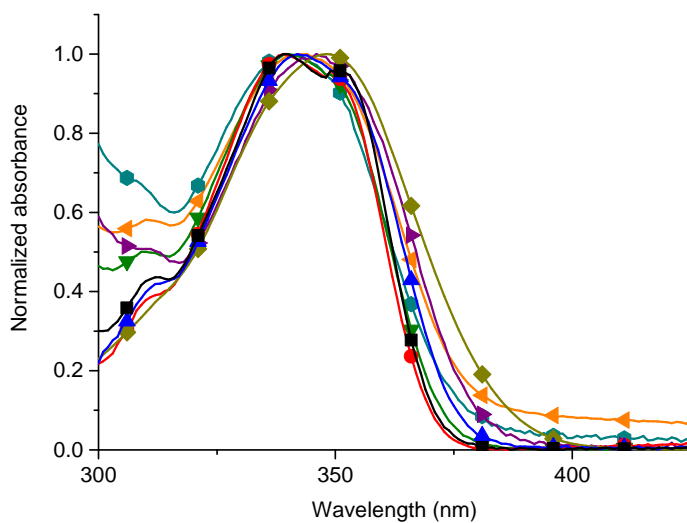


Figure S1. Normalized absorbance spectra of **1** in toluene (■), ether (●), tetrahydrofuran (▲), ethyl acetate (▼), chloroform (▶), dichloromethane (◀), acetonitrile (●), and ethanol (◆).

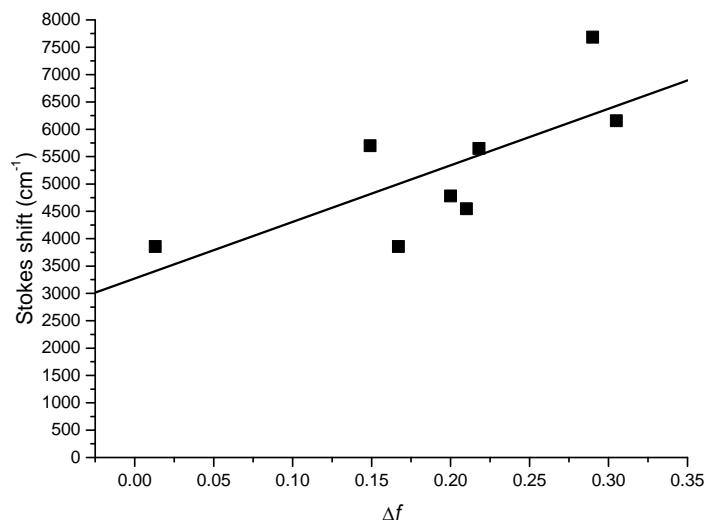


Figure S2. Lippert-Mataga plot showing the Stokes shift of **1** as a function of the solvent orientation polarizability ( $\Delta f$ ).

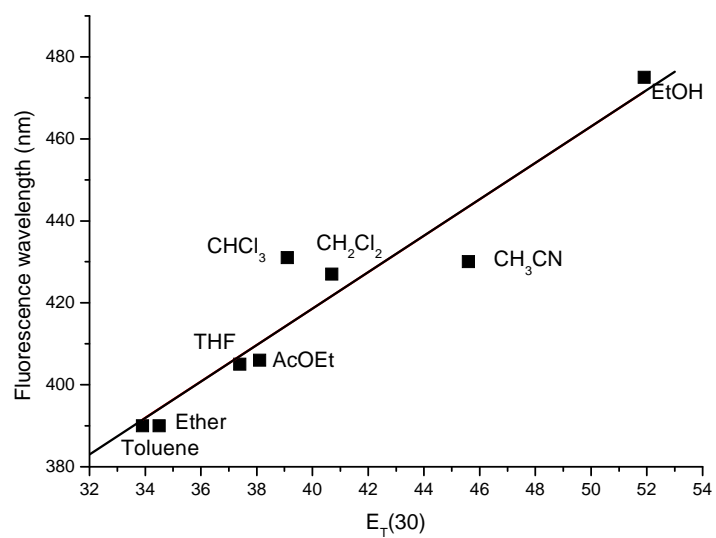


Figure S3. Uncorrected fluorescence of **1** as a function of  $E_T(30)$  in various solvents.

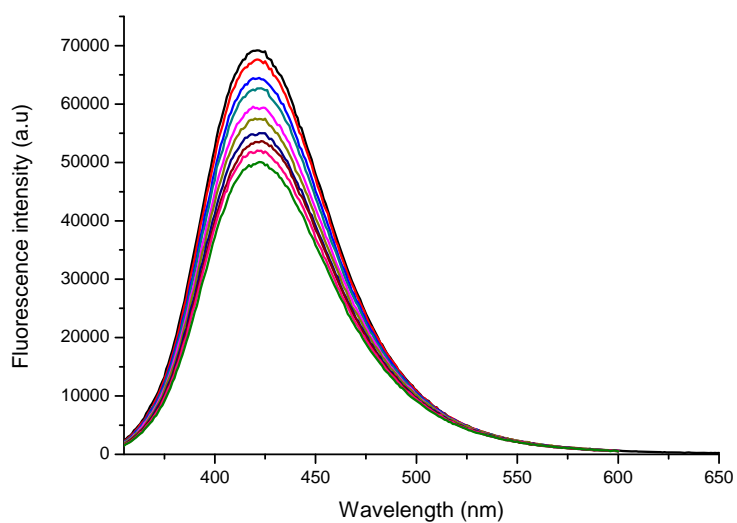


Figure S4. Uncorrected fluorescence quenching of **1** as a function of nitrobenzene concentration from 0 (—) to 1 (—) mM.

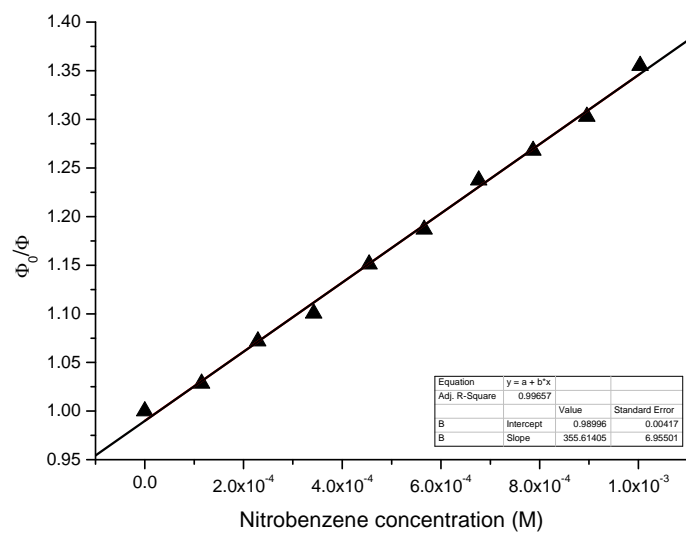


Figure S5. Stern-Volmer quenching of **1** as a function of nitrobenzene.

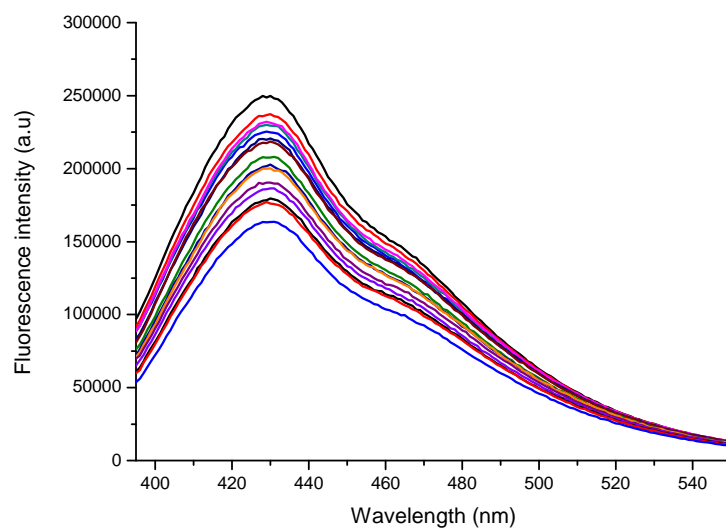


Figure S6. Uncorrected fluorescence quenching of **1** as a function of 2,6-dinitrotoluene concentration from 0 (—) to 2.2 (—) mM.

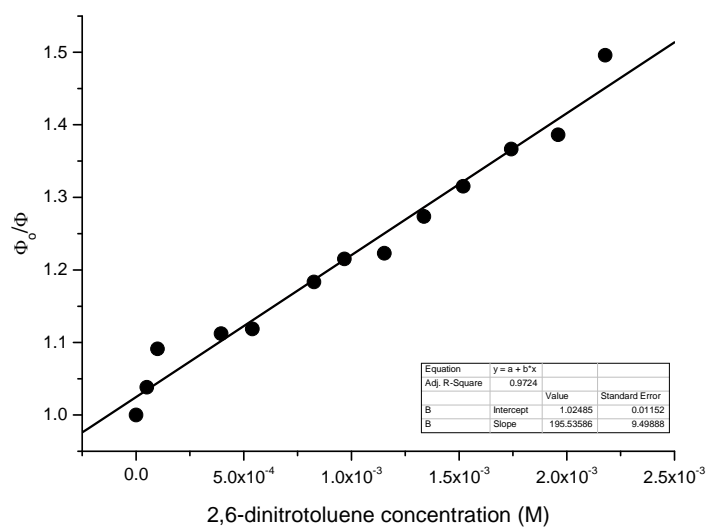


Figure S7. Stern-Volmer quenching of **1** as a function of 2,6-dinitrotoluene.

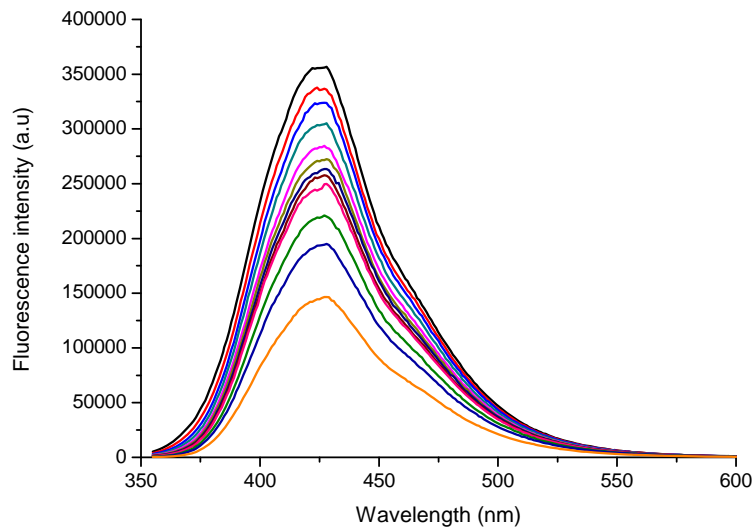


Figure S8. Uncorrected fluorescence quenching of **1** as a function of nitromethane concentration from 0 (—) to 250 (—) mM.

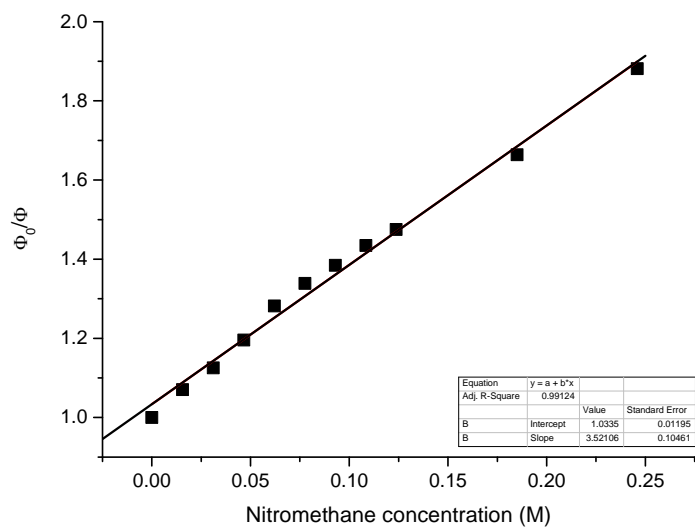


Figure S9. Stern-Volmer quenching of **1** as a function of nitromethane.

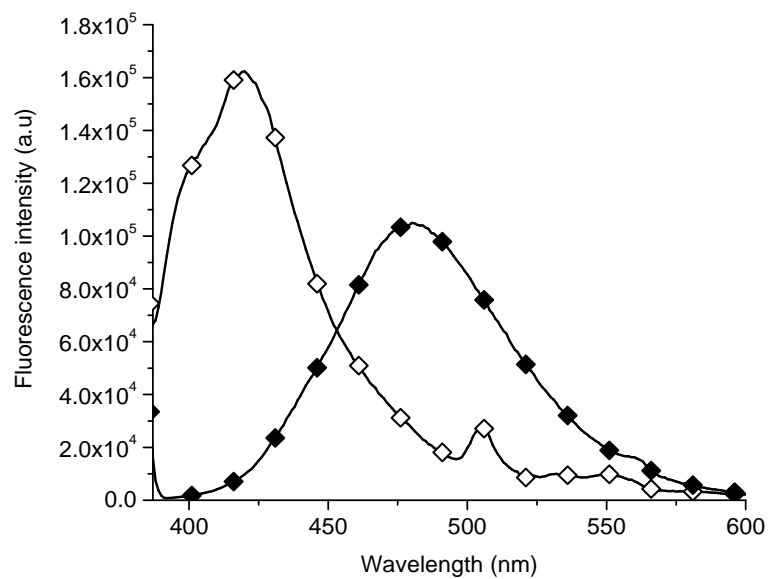


Figure S10. Temperature dependent uncorrected fluorescence of **1** in ethanol/methanol (4:1) at 300 K (◆) and 77 K (◇).

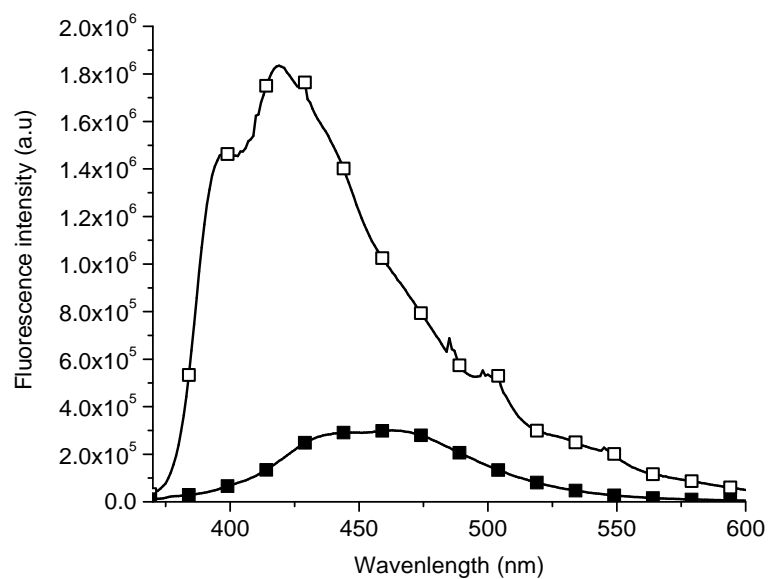


Figure S11. Temperature dependent uncorrected fluorescence of **1** in methylcyclohexane at 300 K (■) and 77 K (□).

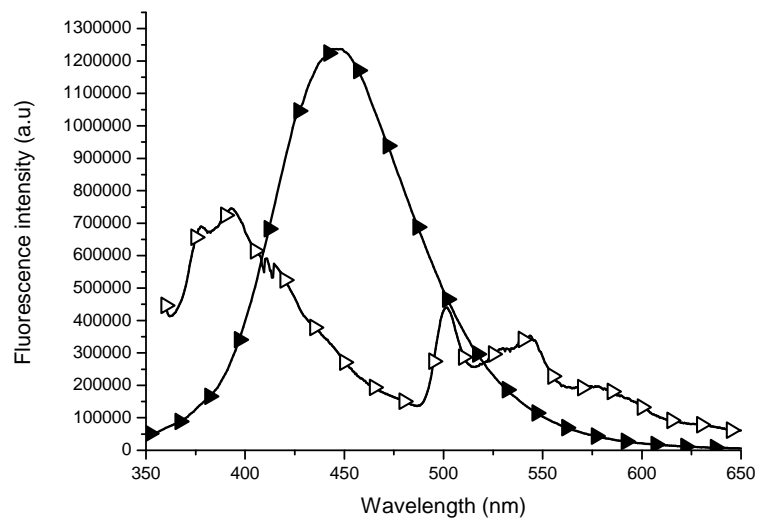


Figure S12. Temperature dependent uncorrected fluorescence of **1** in ether/pentane/EtOH (5:5:1) at 300 K (▴) and 77 K (▷).

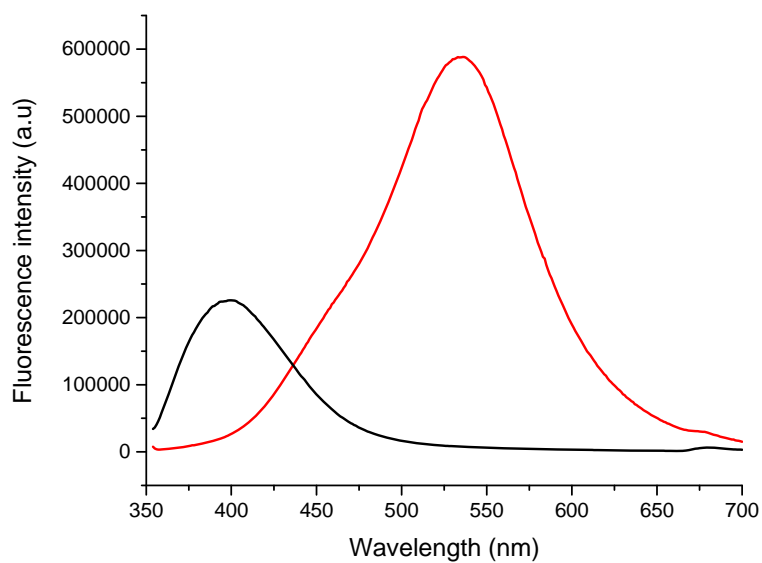


Figure S13. Relative corrected fluorescence of **1** in dichloromethane without (—) and with trifluoroacetic acid (—) added.

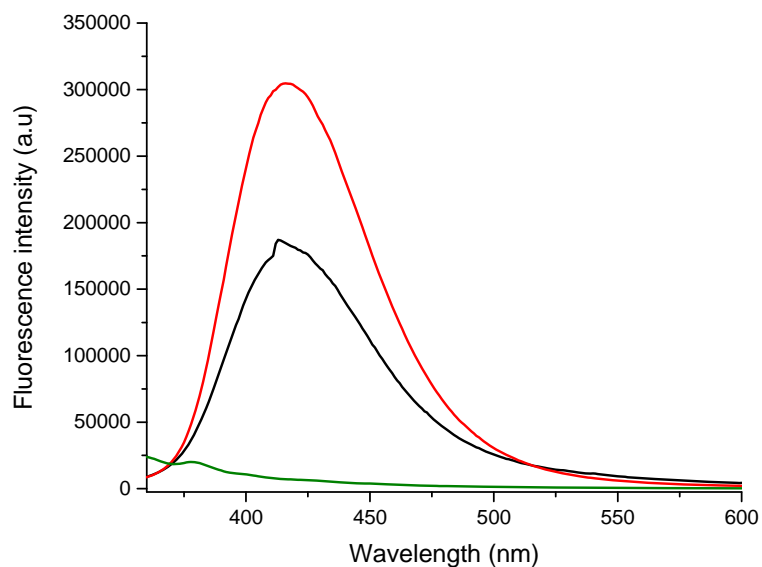


Figure S14. Corrected fluorescence of **1** in dichloromethane (—), chloroform (—), methylcyclohexane (—) excited at 345 nm with matching absorbance at 345 nm measured with identical instrument parameters.

Table S1. Fluorescence lifetimes of **1** measured in various solvents.<sup>a</sup>

Solvent	$\tau_1^b$	$\tau_2$	$\tau_3$	$\chi^2$	Channels <sup>c</sup>
Methylcyclohexane	0.14 (30.2)	1.02 (64.3)	7.08 (5.5)	1.277	0 to 1433
Toluene	0.07 (59.7)	0.97 (38.2)	3.09 (2.1)	0.999	0-2024
Tetrahydrofuran	0.07 (50.9)	0.94 (42.1)	2.64 (6.9)	0.930	286 to 1515
Acetonitrile	0.27 (76.5)	0.61 (22.4)	3.05 (1.12)	1.129	0-2024
Dichloromethane	0.13 (30.2)	0.57 (24.1)	1.98 (2.6)	1.075	0-2024
Ethanol	-	2.54	-	1.010	245 to 1310

<sup>a</sup> Values in parentheses are weighted signal percentage of the corresponding lifetime. <sup>b</sup>Instrument response frequency. <sup>c</sup>Channel number used for decay fitting.

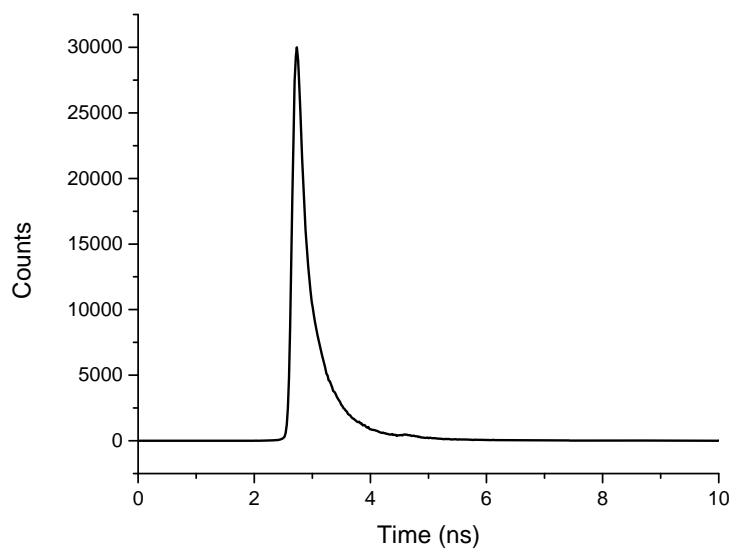


Figure S15. Fluorescence kinetics of **1** monitored at 427 nm in dichloromethane.

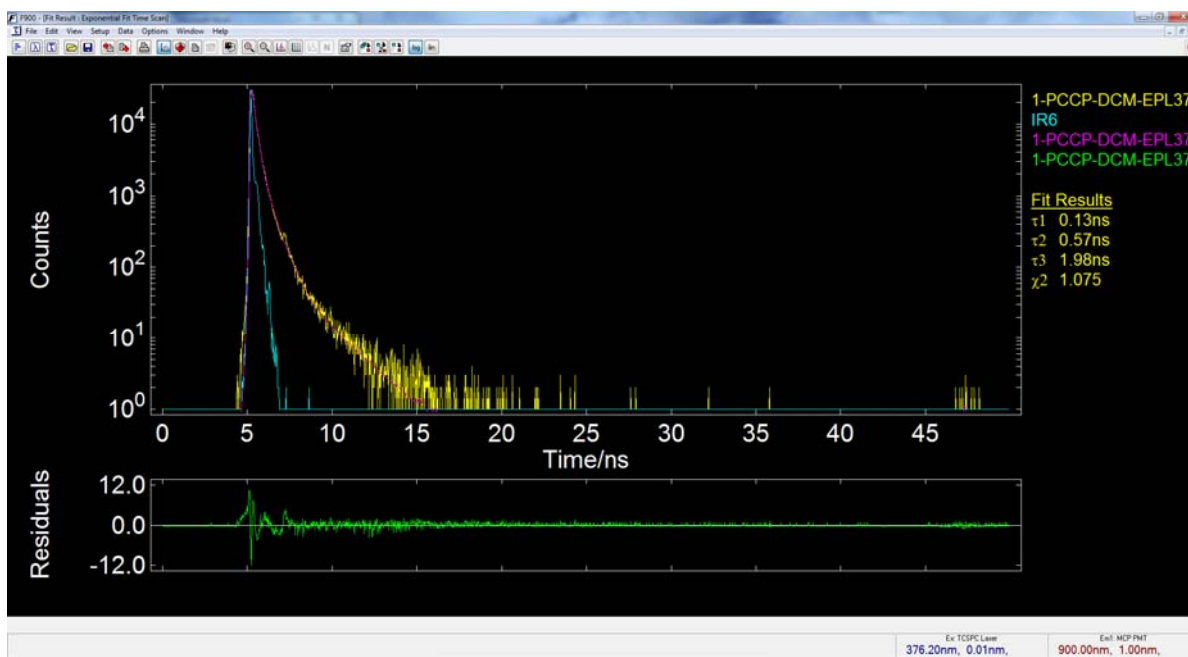


Figure S16. Fluorescence kinetics of **1** monitored at 427 nm in dichloromethane (yellow), instrument response frequency (blue), biexponential numerical fit (pink) taking into account the instrument response frequency, and residual fitting between measured and fitting data (green).

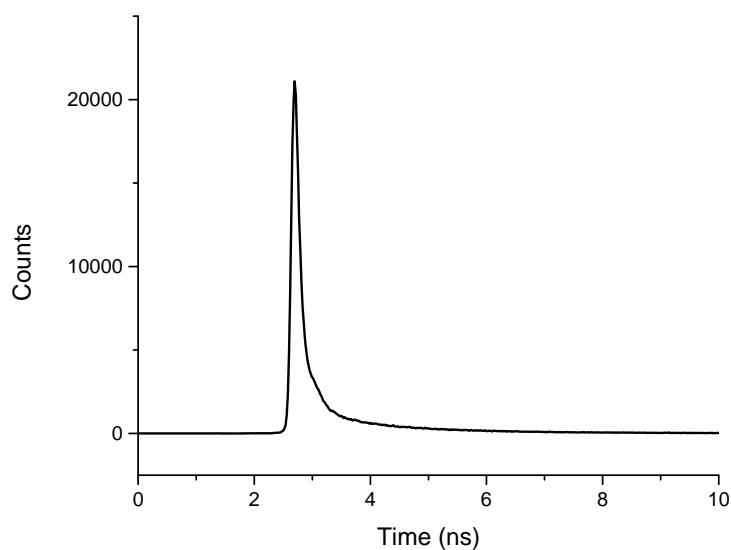


Figure S17. Fluorescence kinetics of **1** monitored at 405 nm in tetrahydrofuran.

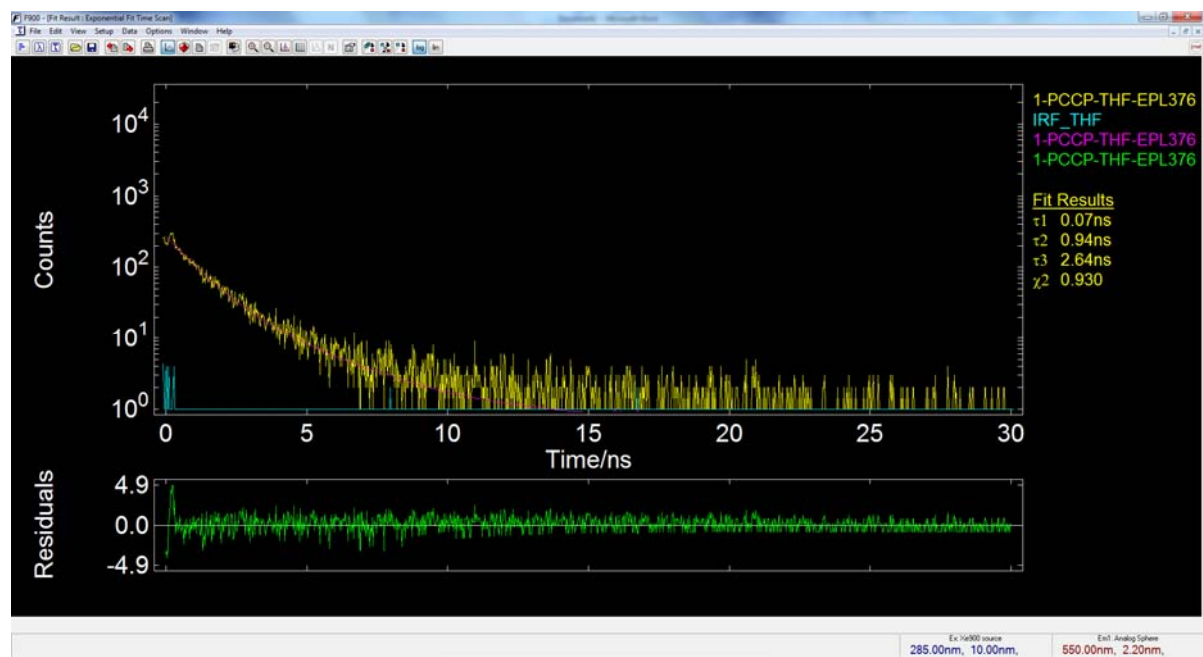


Figure S18. Fluorescence kinetics of **1** monitored at 405 nm in tetrahydrofuran (yellow), instrument response frequency (blue), biexponential numerical fit (pink) taking into account the instrument response frequency, and residual fitting between measured and fitting data (green).

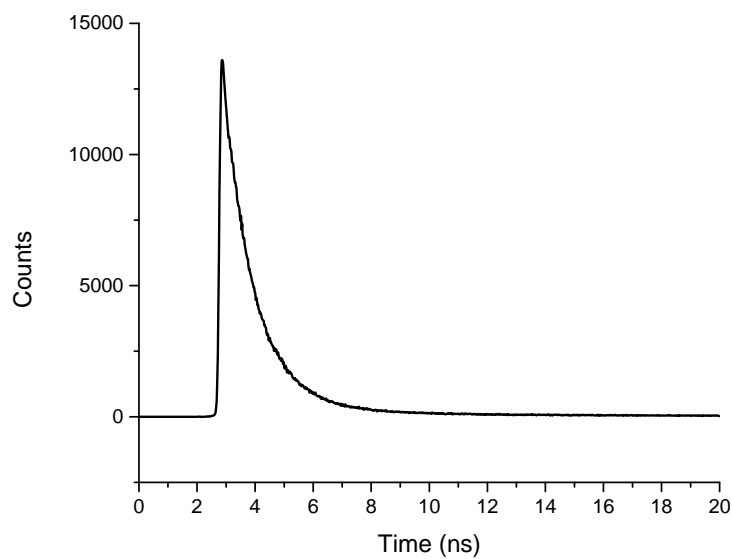


Figure S19. Fluorescence kinetics of **1** monitored at 463 nm in methylcyclohexane.

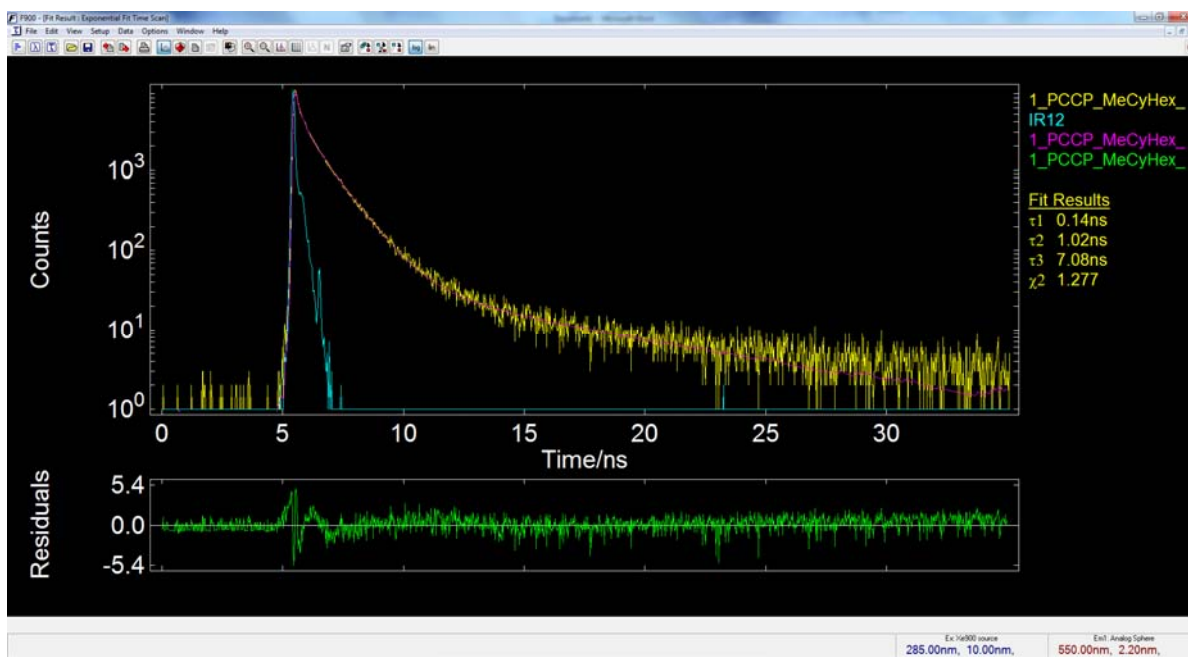


Figure S20. Fluorescence kinetics of **1** monitored at 463 nm in methylcyclohexane (yellow), instrument response frequency (blue), triexponential numerical fit (pink) taking into account the instrument response frequency, and residual fitting between measured and fitting data (green).

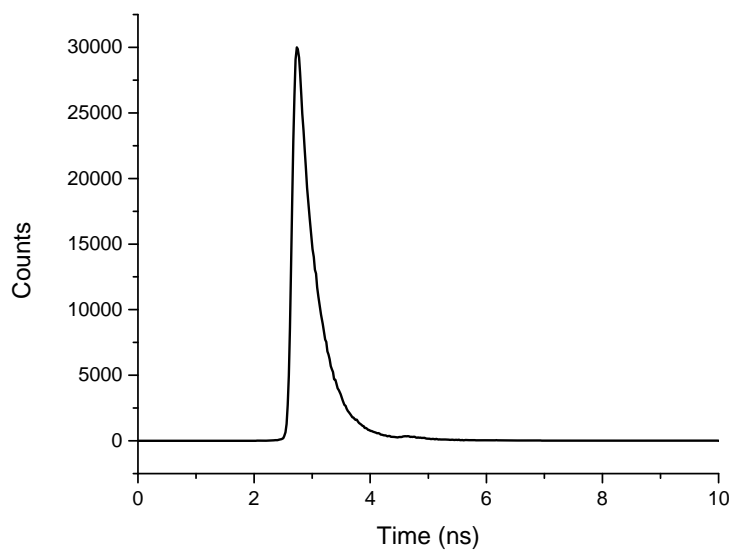


Figure S21. Fluorescence kinetics of **1** monitored at 430 nm in acetonitrile.

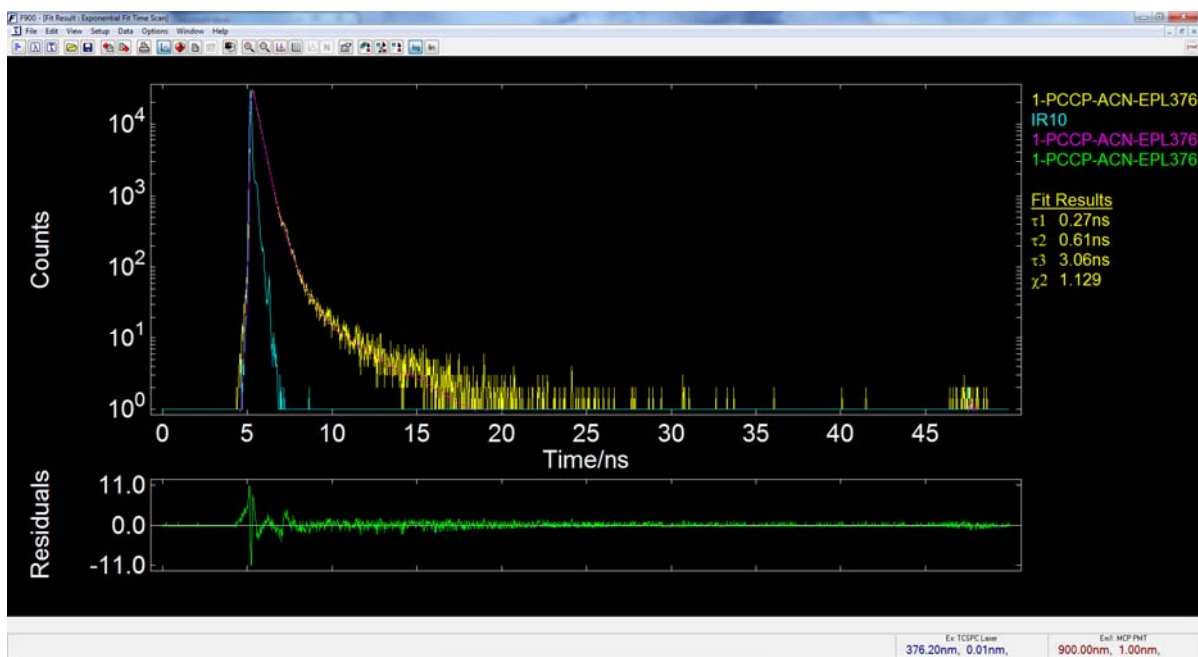


Figure S22. Fluorescence kinetics of monitored **1** at 430 nm in acetonitrile (yellow), instrument response frequency (blue), triexponential numerical fit (pink) taking into account the instrument response frequency, and residual fitting between measured and fitting data (green).

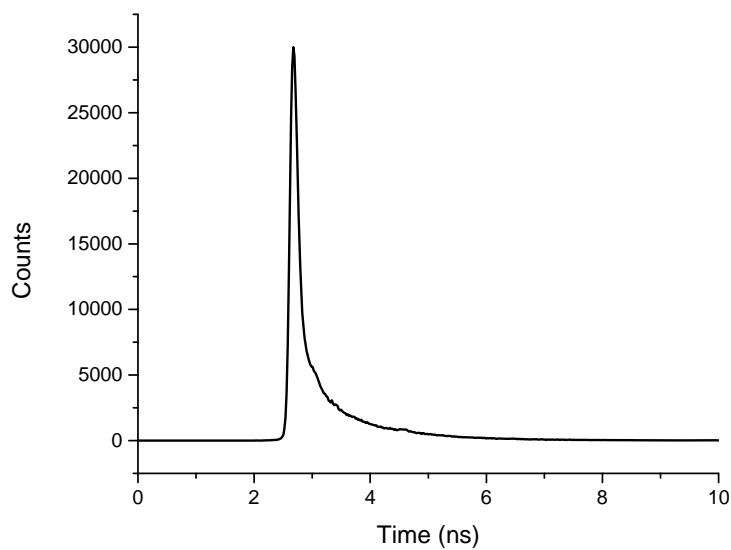


Figure S23. Fluorescence kinetics of **1** monitored at 390 nm in toluene.

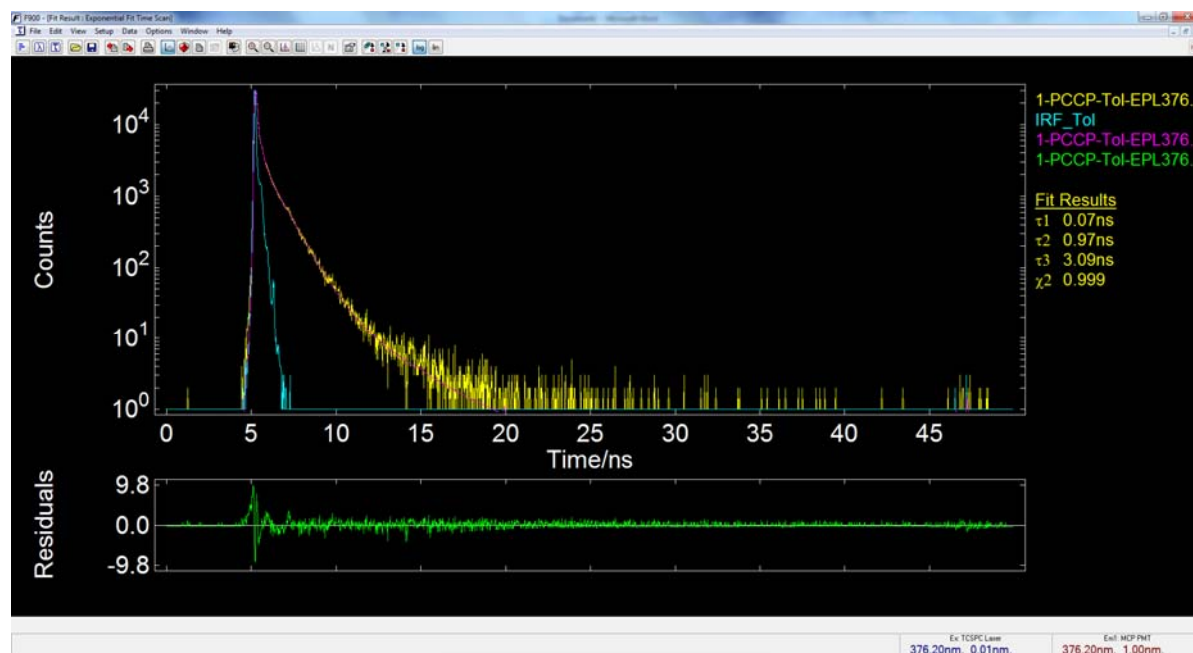


Figure S24. Fluorescence kinetics of **1** monitored at 390 nm in toluene (yellow), instrument response frequency (blue), triexponential numerical fit (pink) taking into account the instrument response frequency, and residual fitting between measured and fitting data (green).

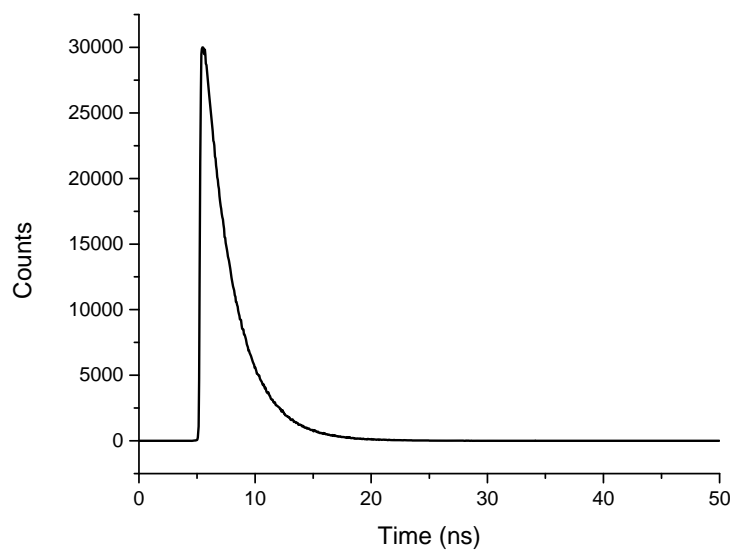


Figure S25. Fluorescence kinetics of **1** monitored at 475 nm in ethanol.

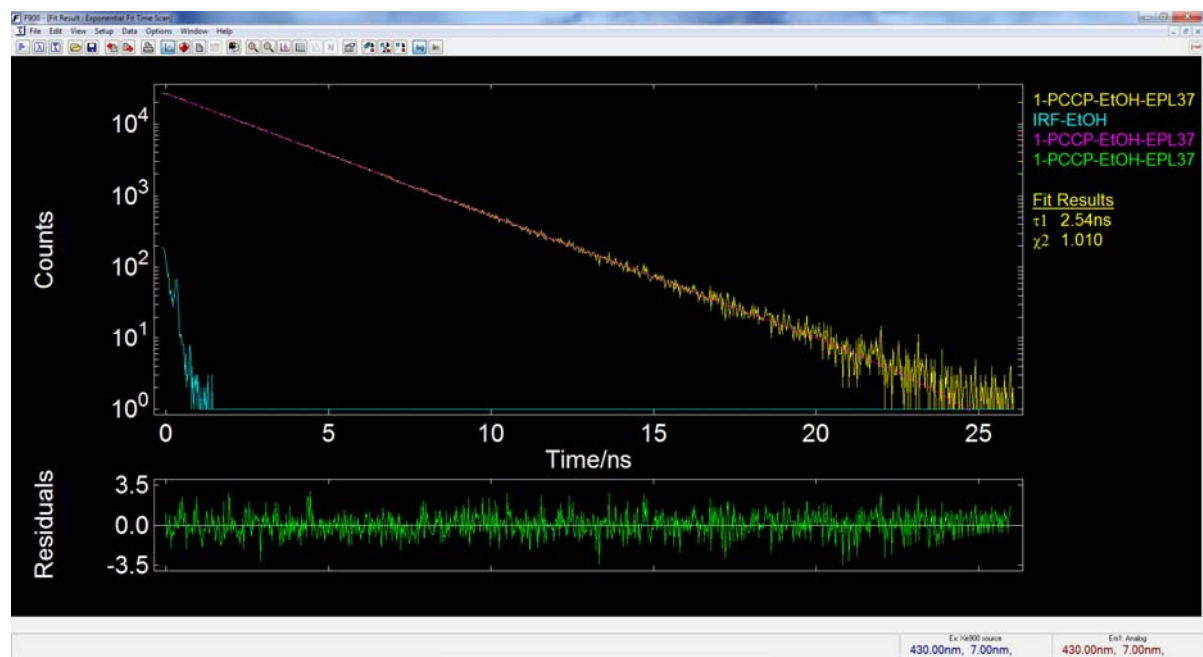


Figure S26. Fluorescence kinetics of **1** monitored at 475 nm in ethanol (yellow), instrument response frequency (blue), monoexponential numerical fit (pink) taking into account the instrument response frequency, and residual fitting between measured and fitting data (green), truncated from 6 to 33 ns.

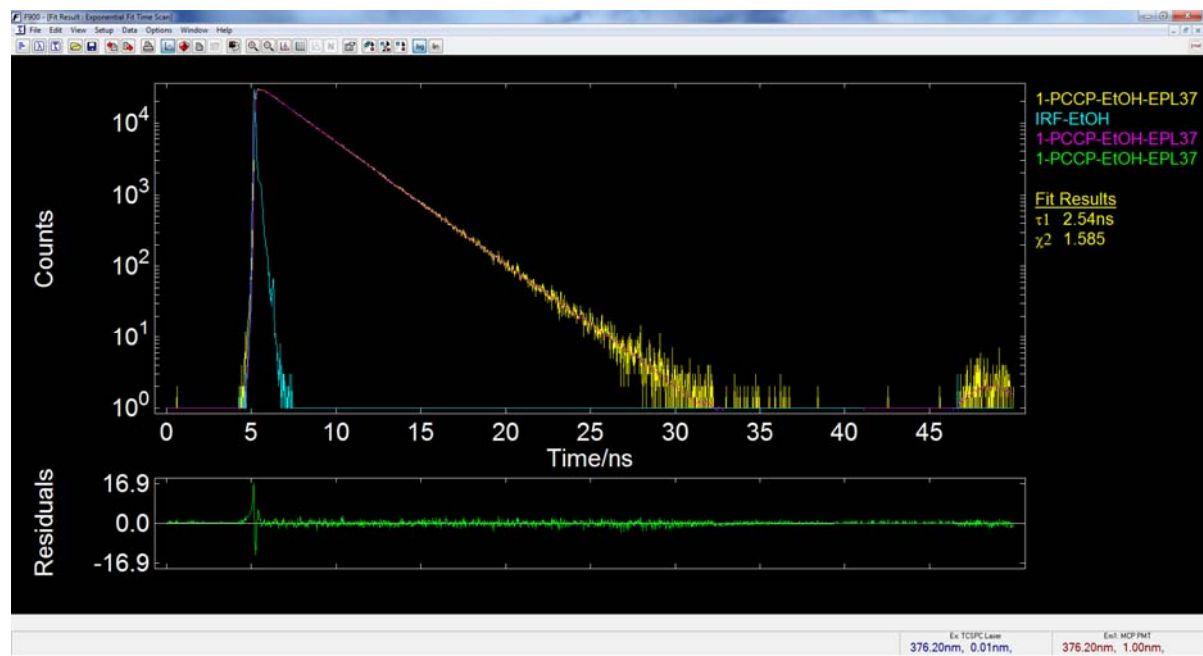


Figure S27. Fluorescence kinetics of **1** monitored at 475 nm in ethanol (yellow), instrument response frequency (blue), monoexponential numerical fit (pink) taking into account the instrument response frequency, and residual fitting between measured and fitting data (green).

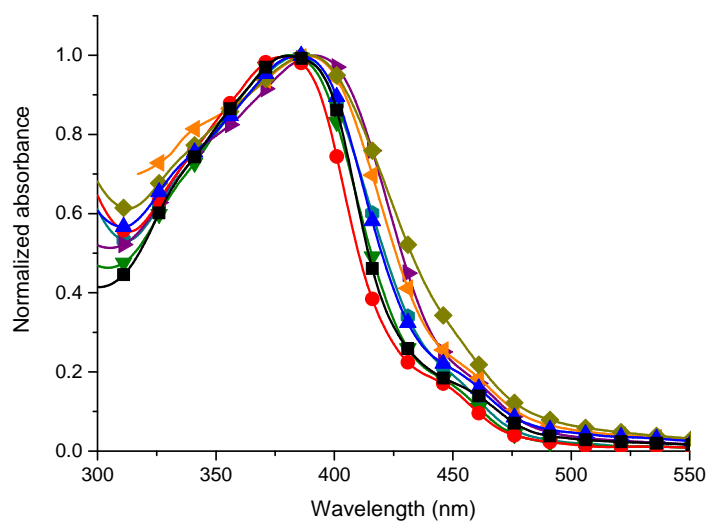


Figure S28. Normalized absorbance spectra of **2** in toluene (■), ether (●), tetrahydrofuran (▲), ethyl acetate (▼), chloroform (▶), dichloromethane (◀), acetonitrile (⬢), and ethanol (◆).

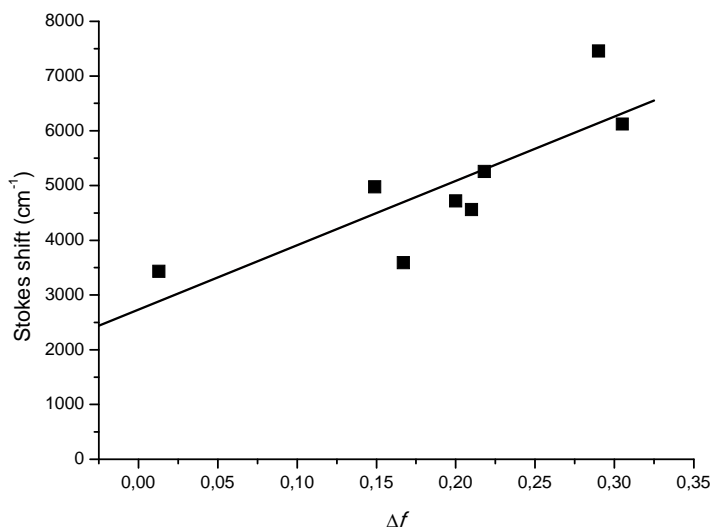


Figure S29. Lippert-Mataga plot showing the Stokes shift of **2** as a function of solvent orientation polarizability ( $\Delta f$ ).

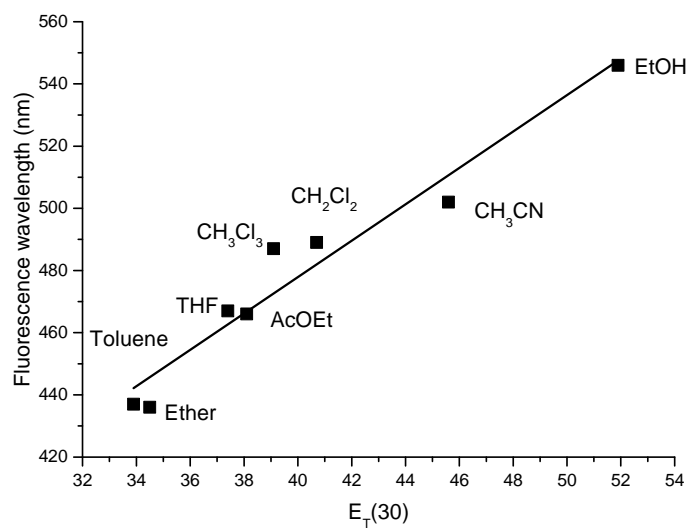


Figure S30. Fluorescence of **2** as a function of  $E_T(30)$  in various solvents.

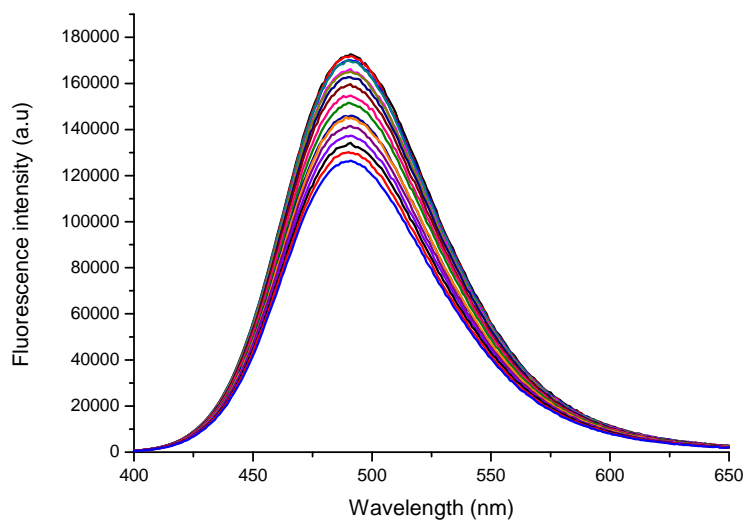


Figure S31. Uncorrected fluorescence quenching of **2** as a function of nitrobenzene concentration from 0 (—) to 2.7 (—) mM.

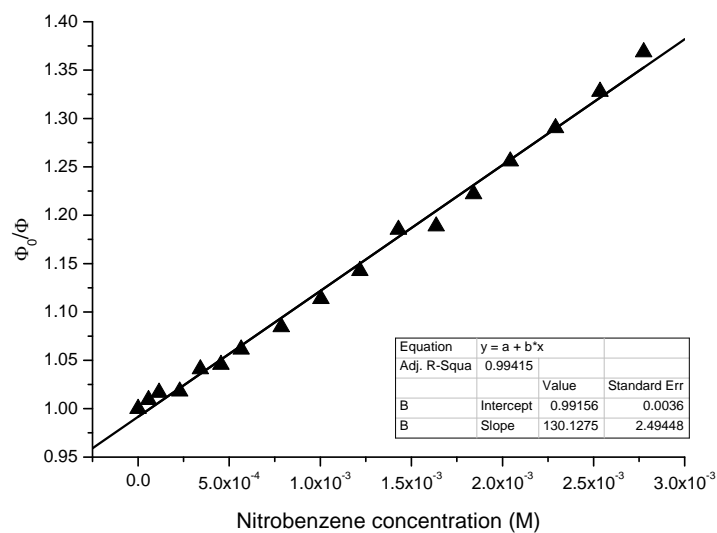


Figure S32. Stern-Volmer quenching of **2** as a function of nitrobenzene.

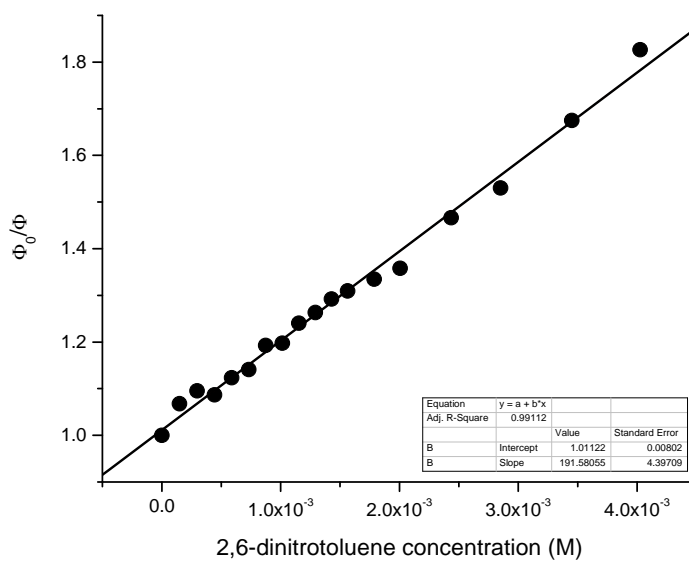


Figure S33. Stern-Volmer quenching of **2** as a function of 2,6-dinitrotoluene.

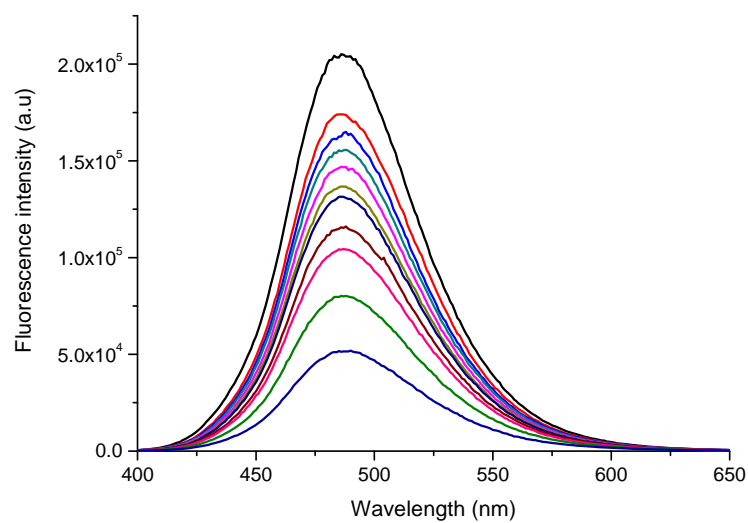


Figure S34. Uncorrected fluorescence quenching of **2** as a function of nitromethane concentration from 0 (—) to 160 (—) mM.

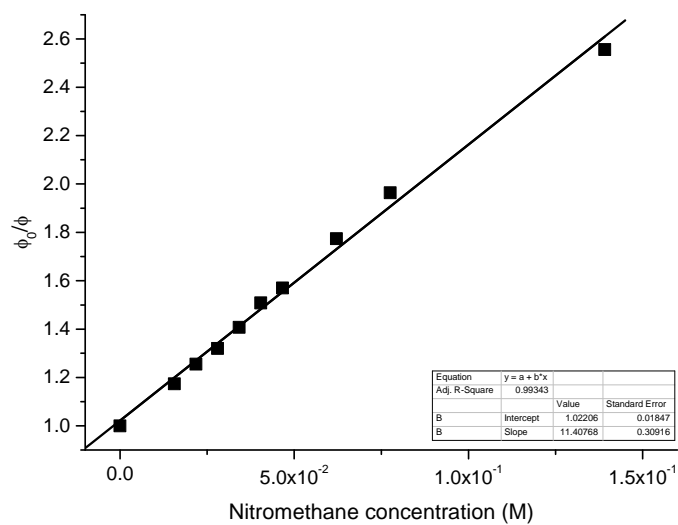


Figure S35. Stern-Volmer quenching of **2** as a function of nitromethane.

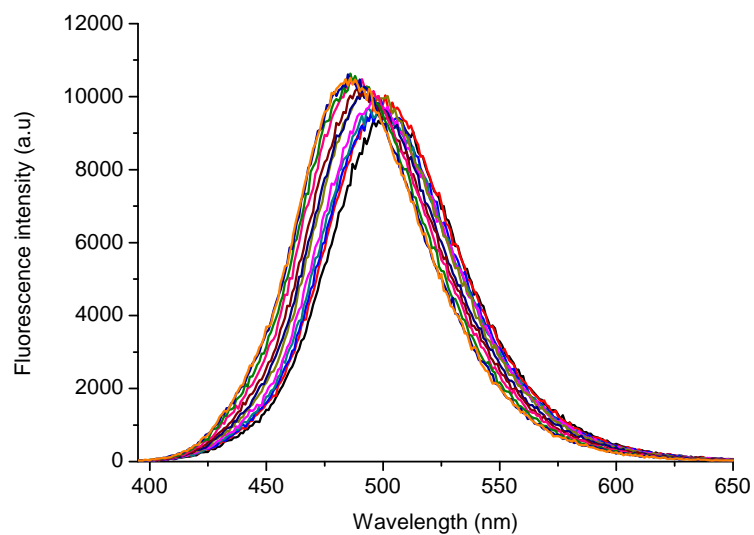


Figure S36. Temperature dependent uncorrected fluorescence of **2** in dichloromethane between 300 K (—) and 190 K (—).

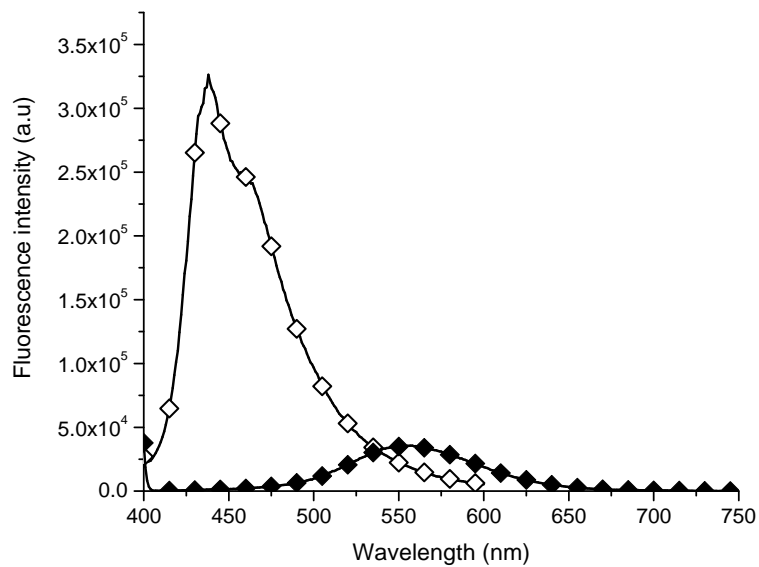


Figure S37. Temperature dependent uncorrected fluorescence of **2** in ethanol/methanol (4:1) at 300 K (◆) and 77 K (◇).

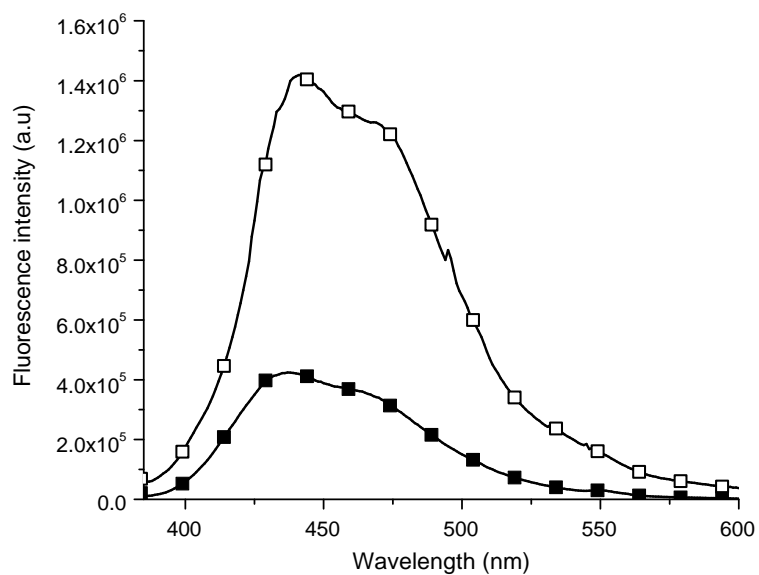


Figure S38. Temperature dependent uncorrected fluorescence of **2** in methylcyclohexane at 300 K (■) and 77 K (□).

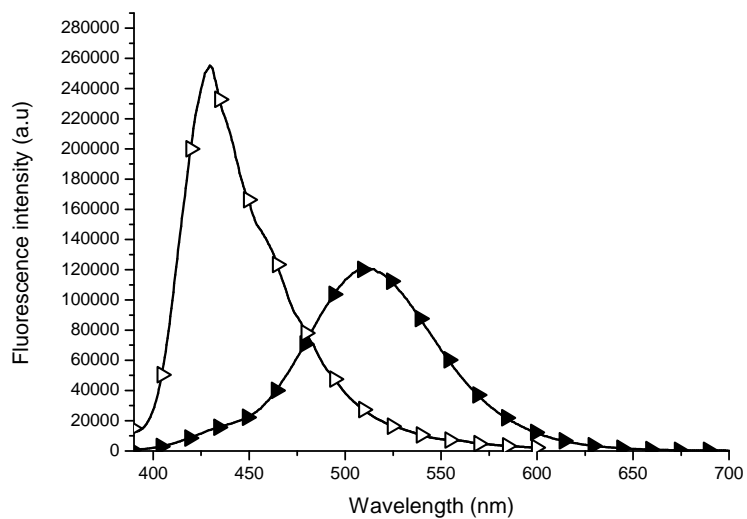


Figure S39. Temperature dependent uncorrected fluorescence of **2** in ether/pentane/EtOH (5:5:1) at 300 K (▶) and 77 K (▷).

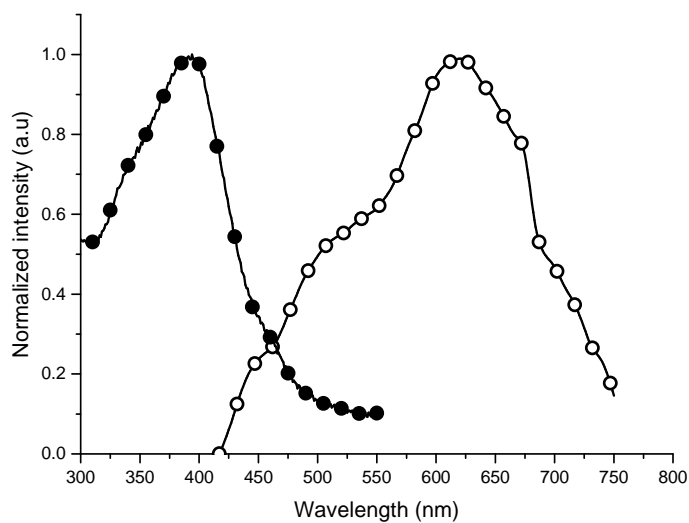


Figure S40. Normalized absorbance (●) and uncorrected fluorescence (○) spectra of **2** deposited as a thin film on a glass substrate.

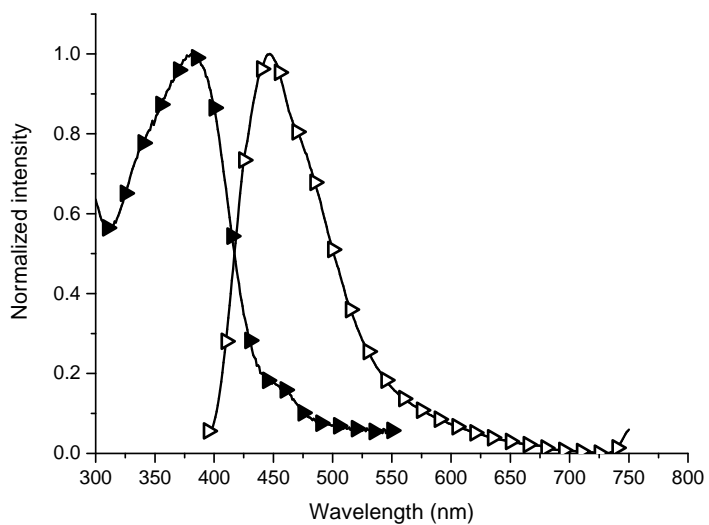


Figure S41. Normalized absorbance (▴) and uncorrected fluorescence (▷) spectra of **2** in a thin film PMMA matrix deposited as a thin film on a glass substrate.

Table S2. Fluorescence lifetimes of **2** measured in various solvents.<sup>a</sup>

Solvent	$\tau_1^b$	$\tau_2$	$\tau_3$	$\chi^2$	Channels <sup>c</sup>
Methylcyclohexane	0.21 (25.5)	0.99 (58.6)	2.55 (15.9)	1.025	143 to 2047
Tetrahydrofuran	1.61 (28.2)	2.48 (71.8)		1.056	180 to 2047
Dichloromethane	0.83 (6.2)	2.42 (93.8)		1.096	333 to 2047
Ethyl acetate	1.21 (19.5)	2.39 (80.5)		1.058	307 to 2047
Ethanol	0.02 (17.9)	2.79 (82.1)		1.038	333 to 2047

<sup>a</sup> Values in parentheses are weighted signal percentage of the corresponding lifetime. <sup>b</sup>Instrument response frequency. <sup>c</sup>Channel number used for decay fitting.

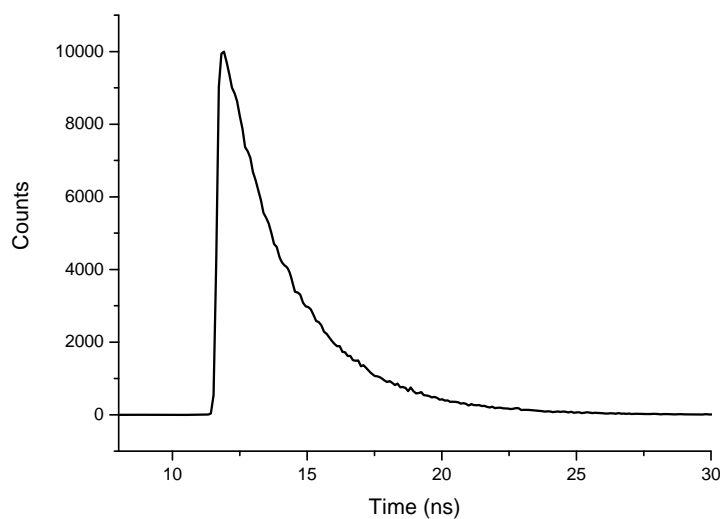


Figure S42. Fluorescence kinetics of **2** monitored at 491 nm in ethanol: methanol (4:1).

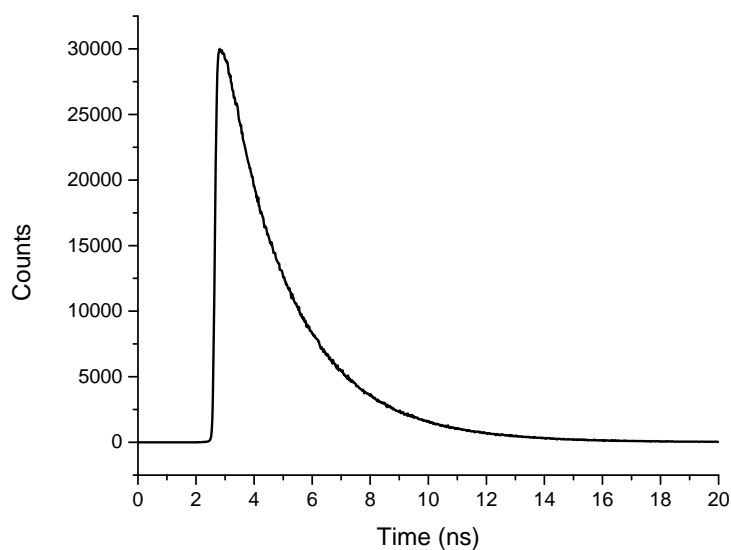


Figure S43. Fluorescence kinetics of **2** monitored at 489 nm in dichloromethane.

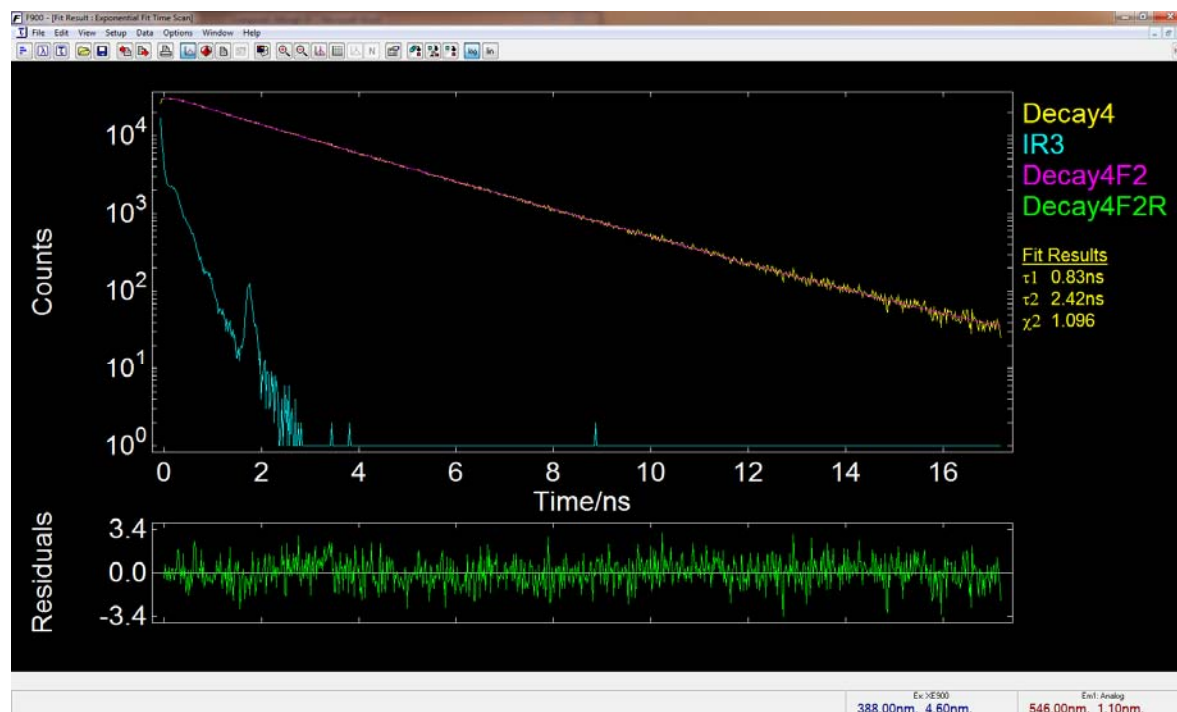


Figure S44. Fluorescence kinetics of **2** monitored at 489 nm in dichloromethane (yellow), instrument response frequency (blue), biexponential numerical fit (pink) taking into account the instrument response frequency, and residual fitting between measured and fitting data (green).

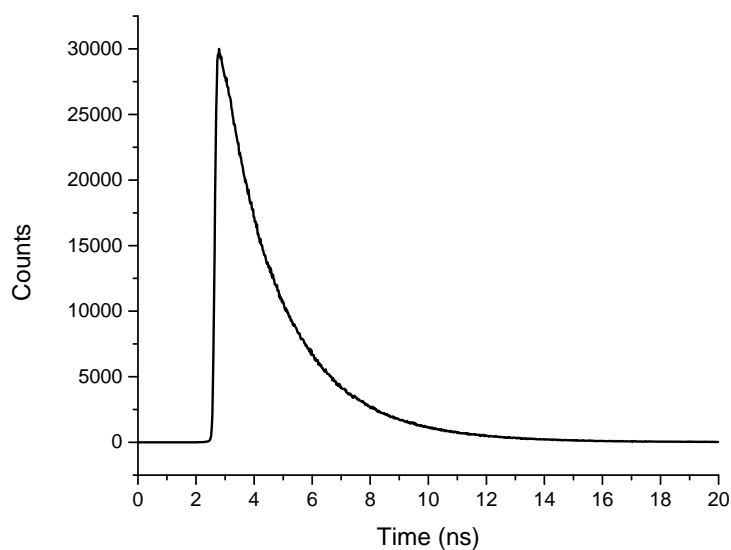


Figure S45. Fluorescence kinetics of **2** monitored at 466 nm in ethyl acetate.

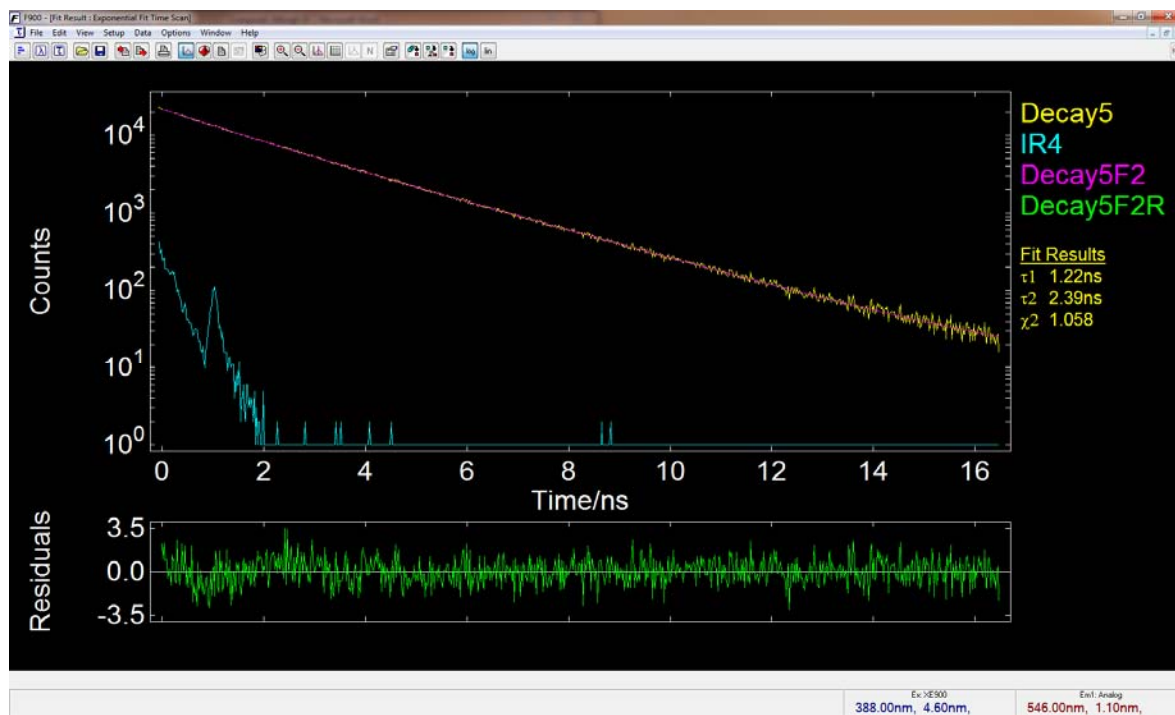


Figure S46. Fluorescence kinetics of **2** monitored at 466 nm in ethyl acetate (yellow), instrument response frequency (blue), biexponential numerical fit (pink) taking into account the instrument response frequency, and residual fitting between measured and fitting data (green).

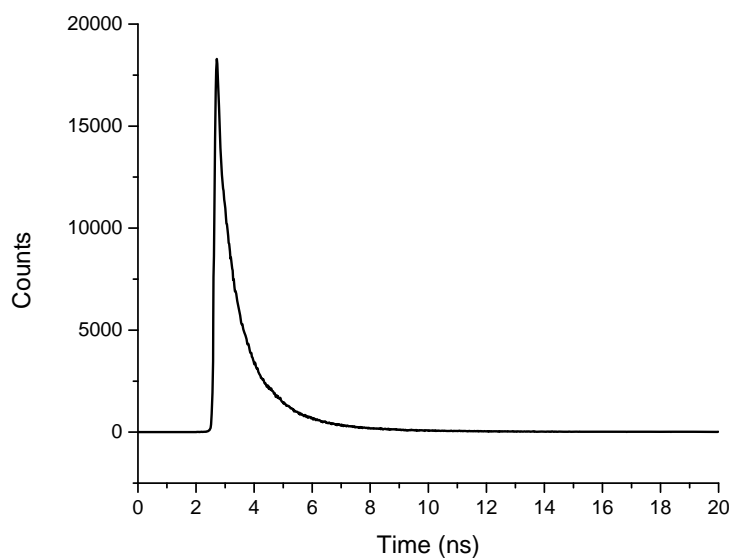


Figure S47. Fluorescence kinetics of **2** monitored at 440 nm in methylcyclohexane.

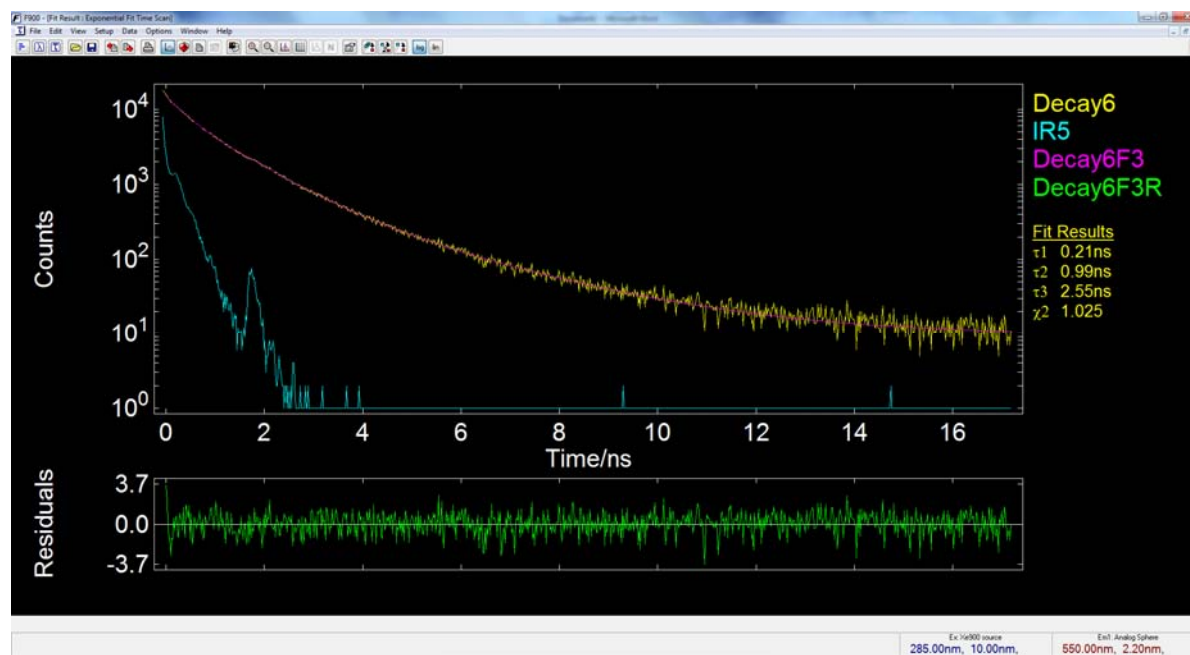


Figure S48. Fluorescence kinetics of **2** monitored at 440 nm in methylcyclohexane (yellow), instrument response frequency (blue), triexponential numerical fit (pink) taking into account the instrument response frequency, and residual fitting between measured and fitting data (green).

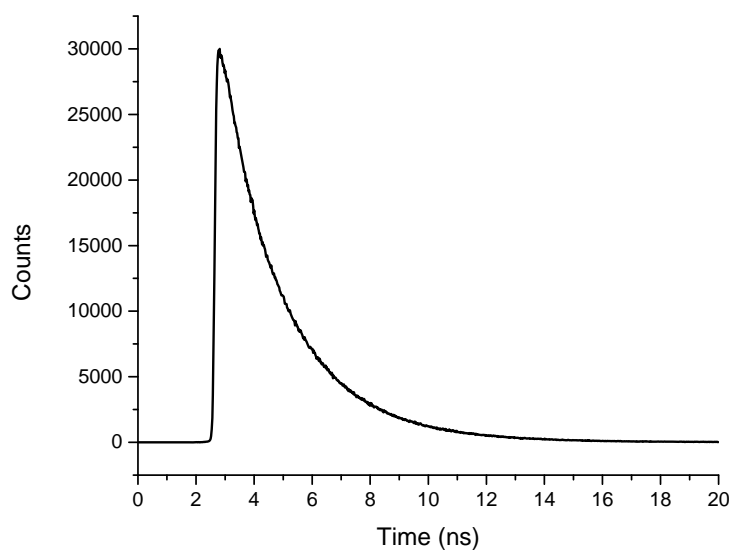


Figure S49. Fluorescence kinetics of **2** monitored at 467 nm in tetrahydrofuran.

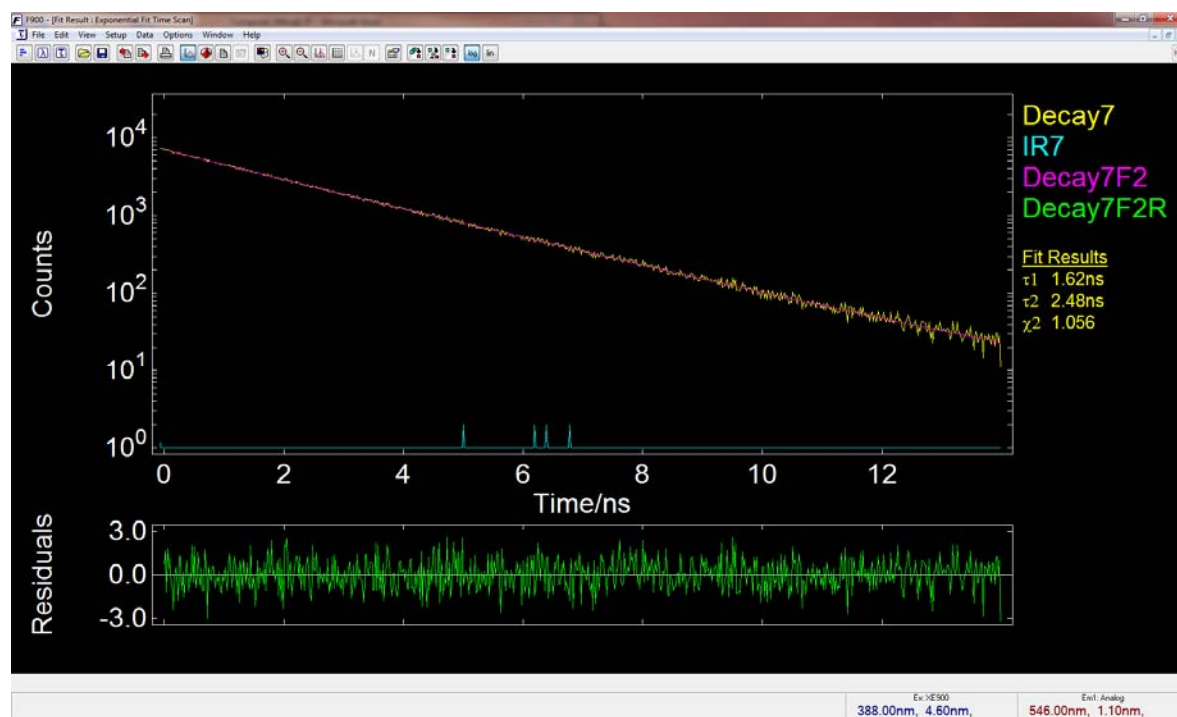


Figure S50. Fluorescence kinetics of **2** monitored at 467 nm in tetrahydrofuran (yellow), instrument response frequency (blue), biexponential numerical fit (pink) taking into account the instrument response frequency, and residual fitting between measured and fitting data (green).

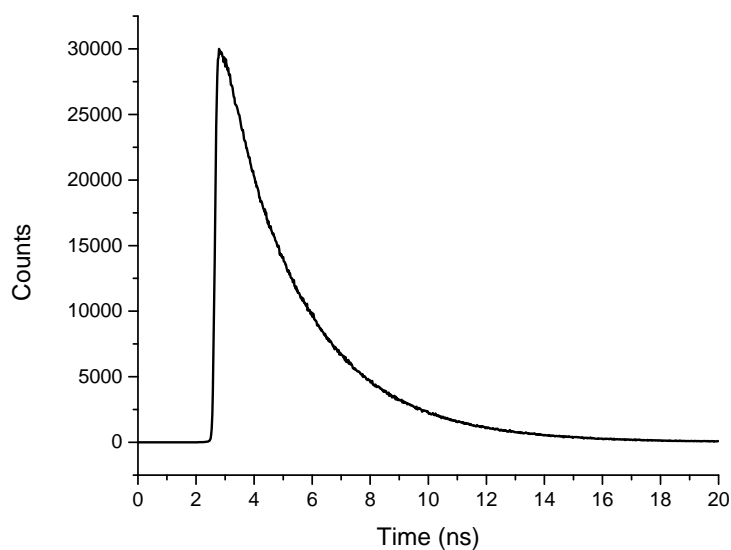


Figure S51. Fluorescence kinetics of **2** monitored at 546 nm in ethanol.

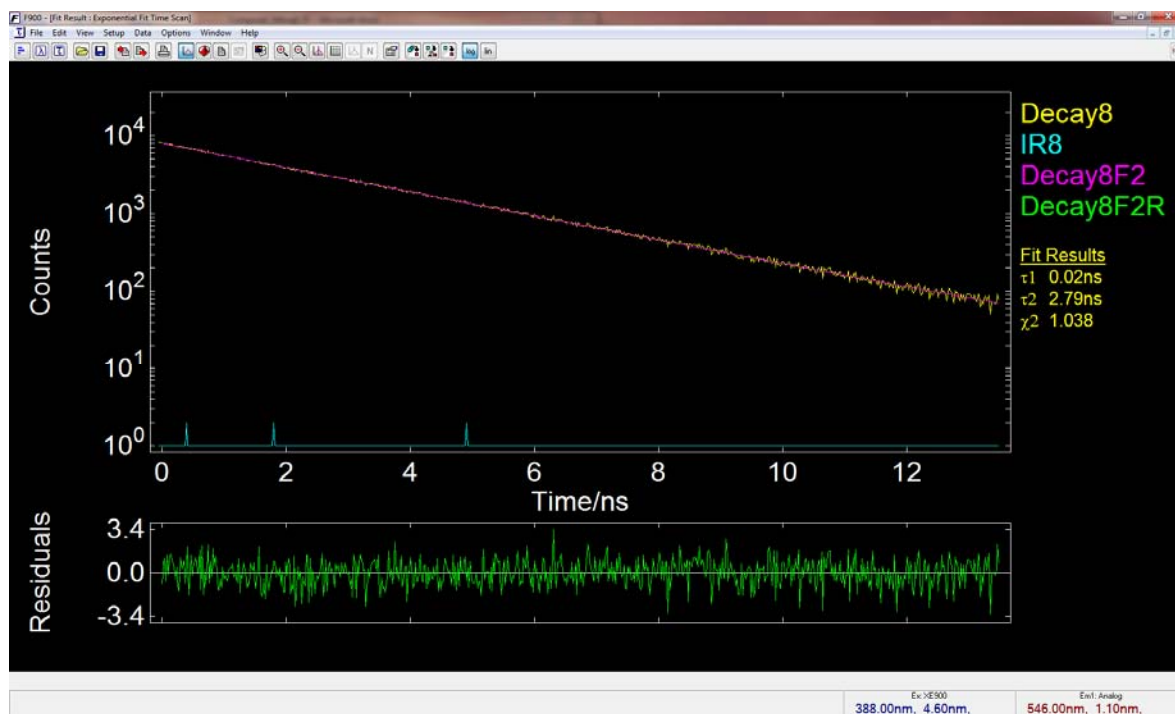


Figure S52. Fluorescence kinetics of **2** monitored at 546 nm in ethanol (yellow), instrument response frequency (blue), biexponential numerical fit (pink) taking into account the instrument response frequency, and residual fitting between measured and fitting data (green).

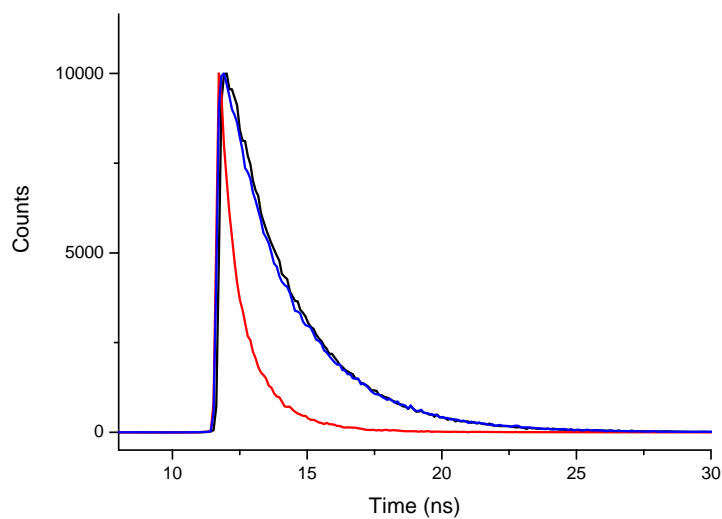


Figure S53. Fluorescence kinetics of **2** monitored at 491 nm in dichloromethane (—), methylcyclohexane (—), and ethanol: methanol (4:1) (—).

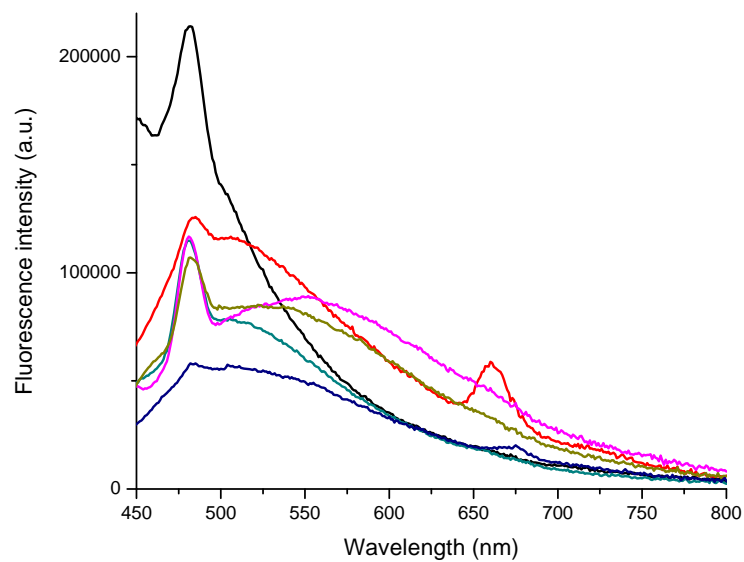


Figure S54. Uncorrected fluorescence spectra of **3** ( $M_n=7200$  g/mol) measured in various solvents: toluene (black), dichloromethane (red), acetonitrile (blue), ether (green), THF (pink), ethyl acetate (olive), chloroform (navy), and ethanol (wine).

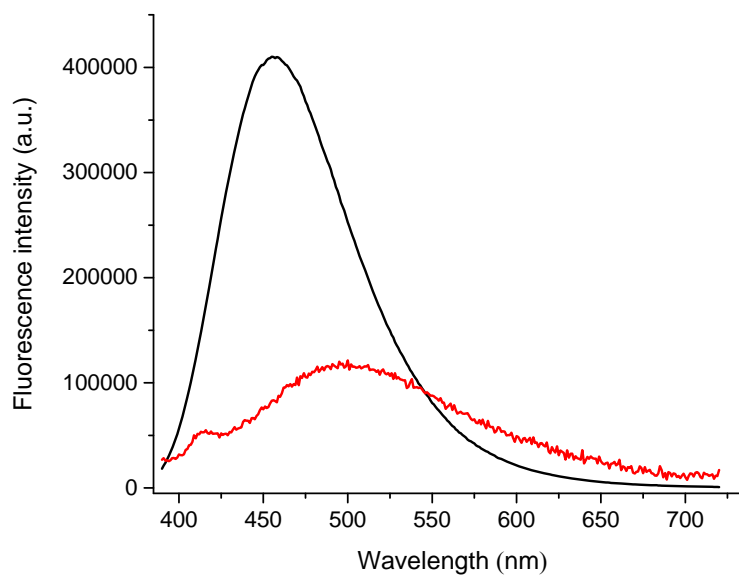


Figure S55. Uncorrected fluorescence spectra of quinine bisulfate in 0.5 M sulfuric acid (black) and **3** (red) magnified 100 times in dichloromethane excited at 370 nm.

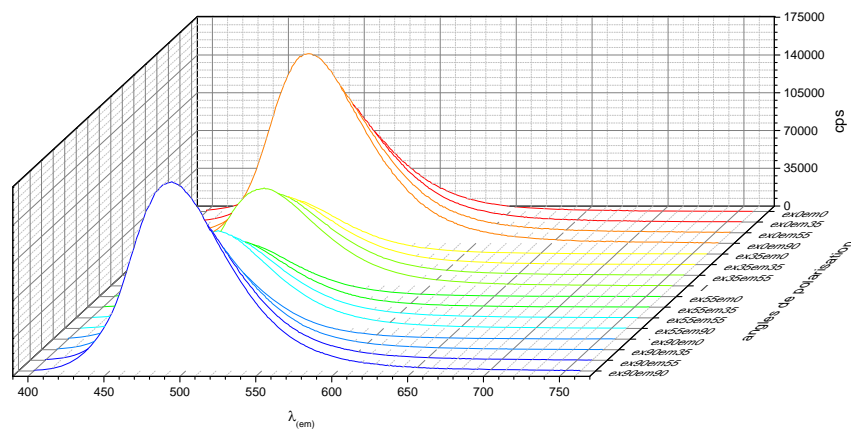


Figure S56. Polarisation fluorescence spectra of **2** measured in dichloromethane.

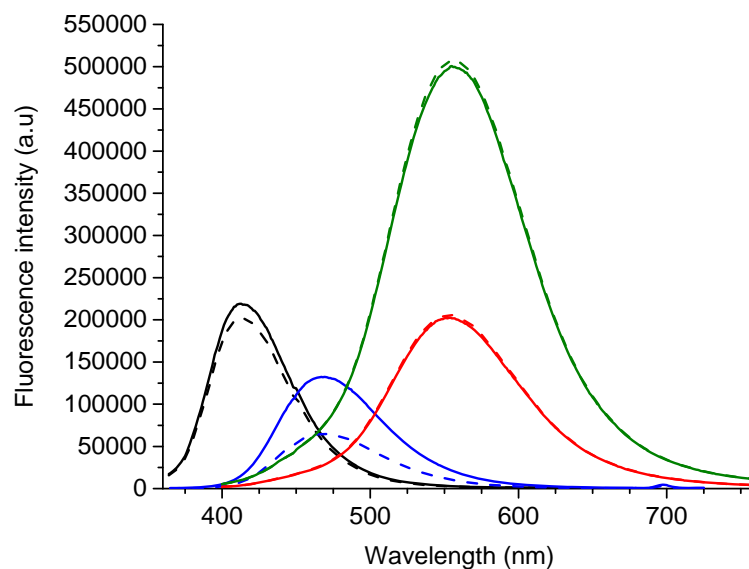


Figure S57. Fluorescence spectra in nitrogen (solid line) and oxygen purged (dashed line) solvents: **1** in dichloromethane (—) and ethanol (—) and **2** in dichloromethane (—) and ethanol (—).

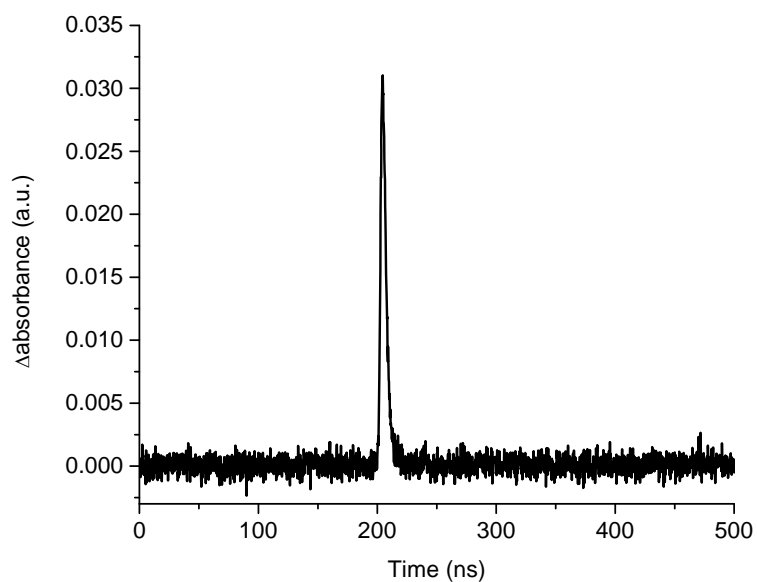


Figure S58. Transient absorbance emission kinetics of **2** monitored at 500 nm with a photomultiplier tube in anhydrous and deaerated dichloromethane after exciting at 423 nm. Fluorescence lifetime is  $6.07 \pm 0.07$  ns.

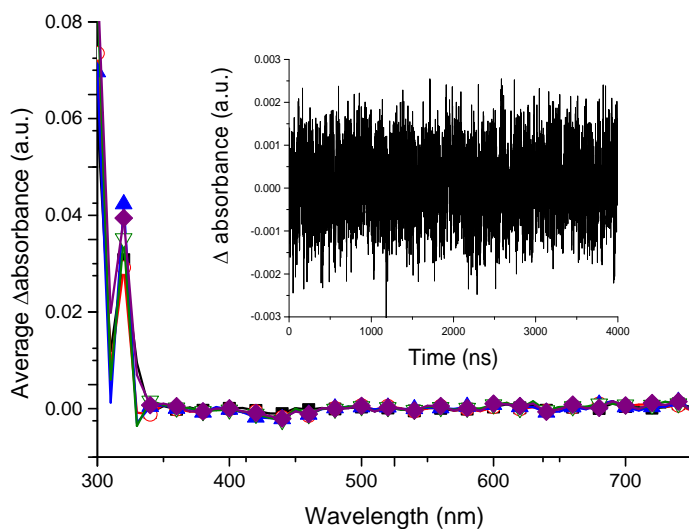


Figure S59. Transient absorbance spectrum of **2** measured in anhydrous and deaerated dichloromethane 0 (■), 800 (○), 1600 (▲), 2400 (▽) and 3200 (◆) ns after exciting at 423 nm. Inset: transient absorbance kinetics of **2** monitored at 500 nm in anhydrous and deaerated dichloromethane after exciting at 423 nm.

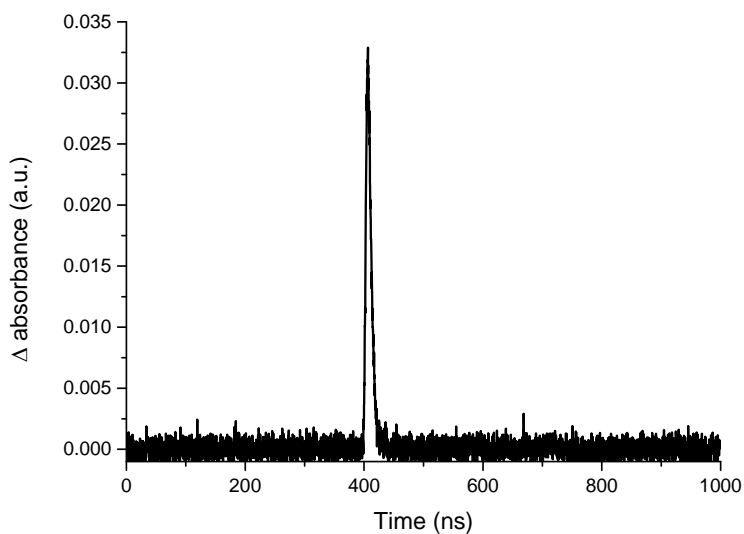


Figure S60. Transient absorbance emission kinetics of **2** monitored at 500 nm with a photomultiplier tube in deaerated tetrahydrofuran after exciting at 423 nm. Fluorescence lifetime is  $5.81 \pm 0.07$  ns.

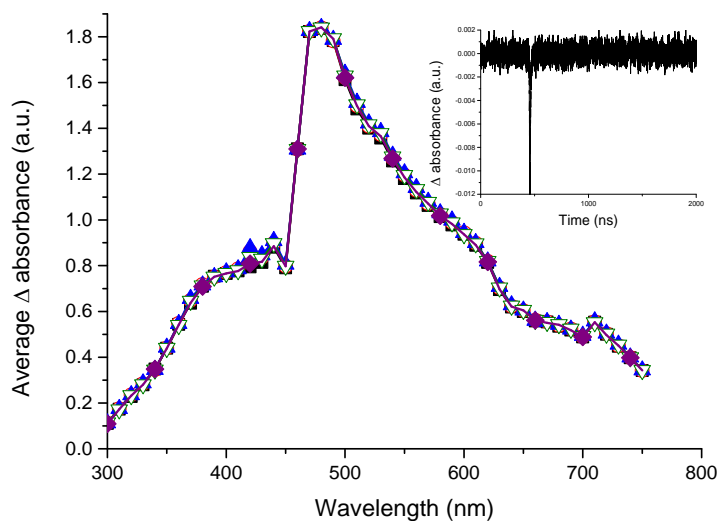


Figure S61. Transient absorbance spectrum of **2** in anhydrous and deaerated tetrahydrofuran 0 (■), 4 (○), 8 (▲), 12 (▽) and 16 (◆) ns after exciting at 423 nm. Inset: transient absorbance kinetics of **2** monitored at 500 nm in anhydrous and deaerated dichloromethane after exciting at 423 nm.

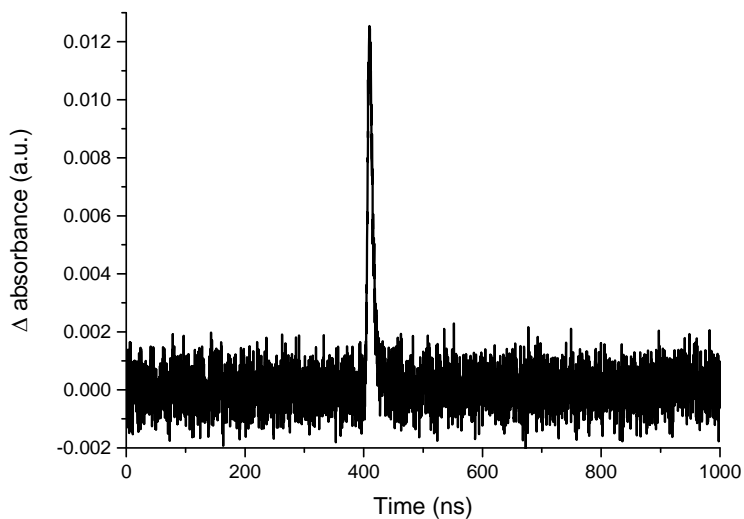


Figure S62. Transient absorbance emission kinetics of **2** monitored at 500 nm with a photomultiplier tube in anhydrous and deaerated toluene after exciting at 423 nm. Fluorescence lifetime is  $5.9 \pm 0.2$  ns.

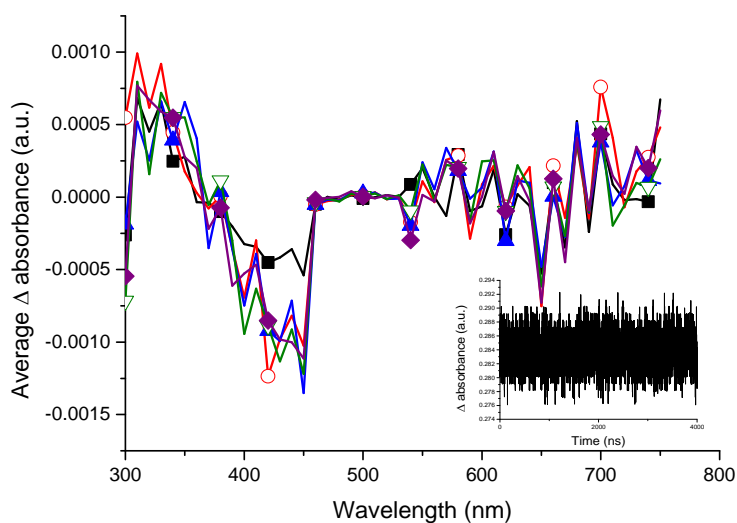


Figure S63. Transient absorbance spectrum of **2** in anhydrous and deaerated toluene after 0 (■), 800 (○), 1600 (▲), 2400 (▽) and 3200 (◆) ns after exciting at 423 nm. Inset: transient absorbance kinetics of **2** monitored at 500 nm in anhydrous and deaerated dichloromethane after exciting at 423 nm.

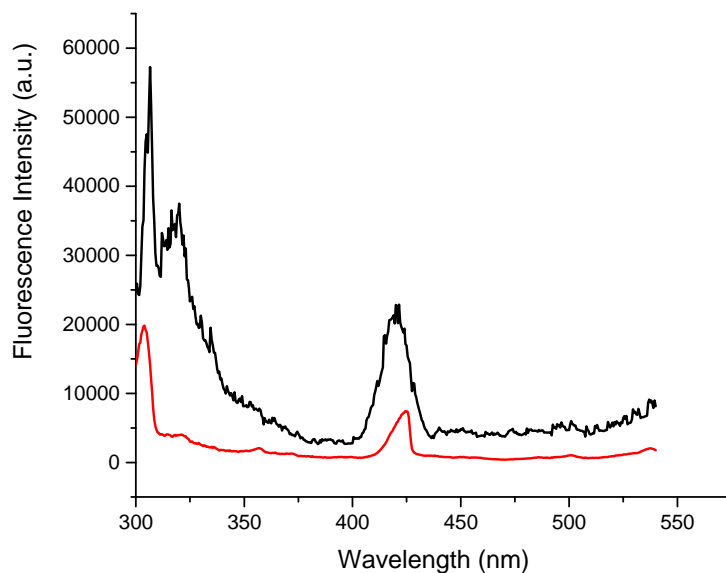


Figure S64. Corrected emission spectra of **3** in toluene at room temperature (red) and 77 K (black) excited at 285 nm.

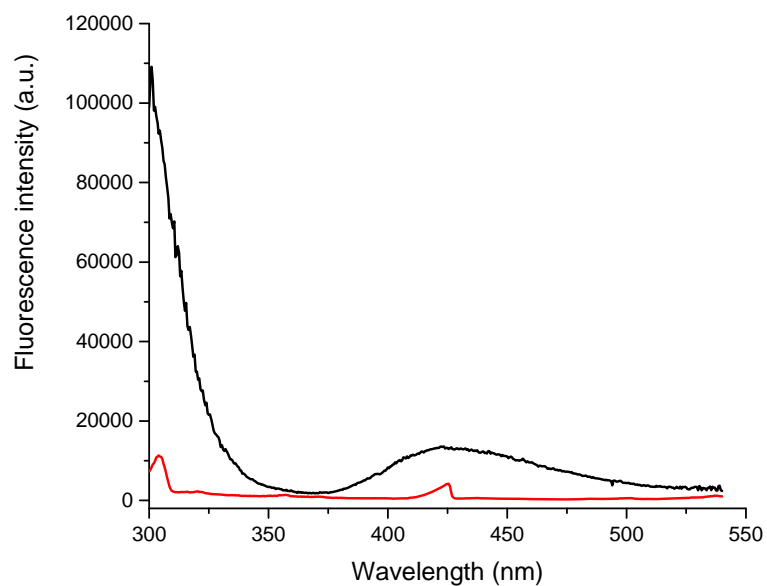


Figure S65. Corrected emission spectra of **3** in 2-methyl-tetrahydrofuran at room temperature (red) and 77 K (black) excited at 285 nm.

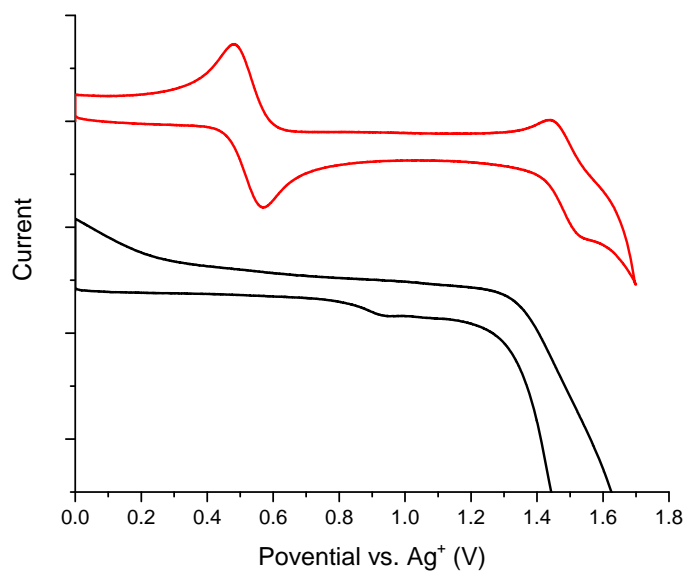
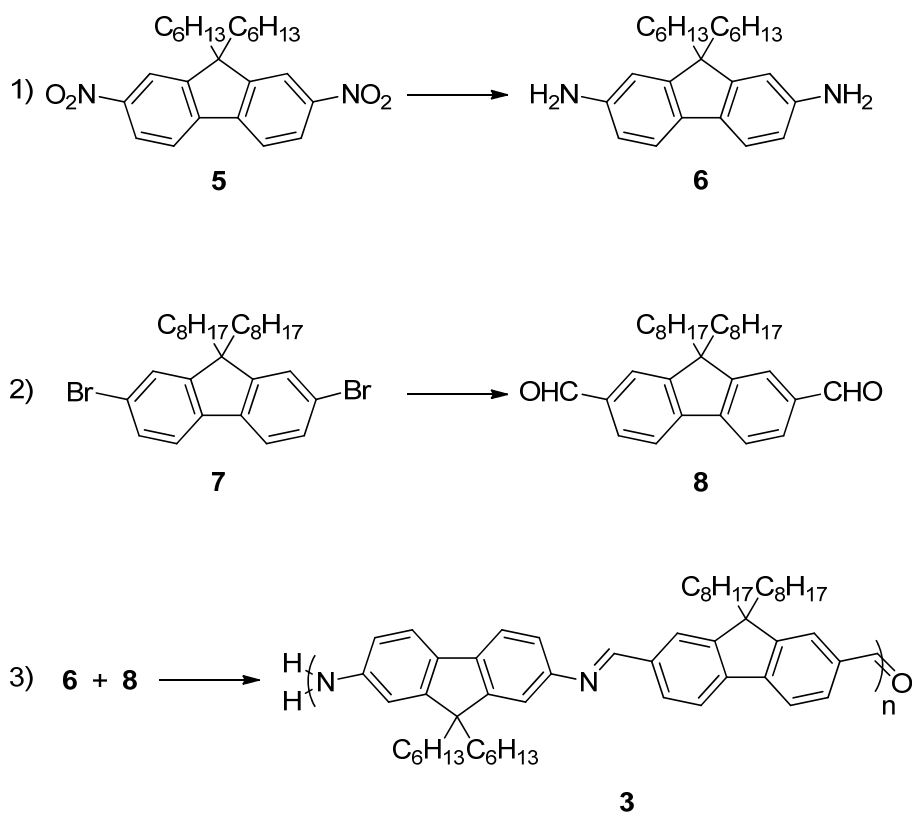


Figure S66. Anodic cyclic voltammograms of **1** (red) and **2** (black) in dichloromethane with  $\text{Bu}_4\text{NPF}_6$  measured with a scan speed of 200 mV/sec. Ferrocene was added to **1** as an internal reference.



Scheme S1. Synthetic scheme for the preparation of **3** and its corresponding monomers.

### Synthesis

**9,9-Dihexyl-2,7-dinitro-9H-fluorene (5).**<sup>1, 2</sup> 9,9-Dihexyl-9H-fluorene (3.8 g, 11 mmol) was dissolved in glacial acetic acid (15 mL) in a 50 mL Schlenk tube equipped with a stir bar. The contents were placed under N<sub>2</sub> and then cooled using a cold water bath. Fuming nitric acid (15 mL) was slowly added to the mixture using a syringe. The mixture was allowed to return to room temperature and was stirred overnight. The contents of the tube were then poured into cold distilled water (100 mL), transferred into a separatory funnel and extracted with ethyl acetate (3 x 50 mL). The organic fraction was washed with distilled water (3 x 50 mL), a saturated aqueous NaHCO<sub>3</sub> solution (3 x 50 mL) and a saturated aqueous NaCl solution (2 x 50 mL), then dried with anhydrous MgSO<sub>4</sub>, filtered, and the solvent was then removed in vacuo. The resulting oil was purified using a silica column. The title compound was obtained as an oily, pale yellow solid (820 mg, 17%). <sup>1</sup>H-NMR (acetone-*d*<sub>6</sub>):  $\delta$  = 8.45 (d, 2H, *J* = 2.0 Hz), 8.36 (dd, 2H, *J* = 8.4 Hz, 2.4

Hz), 8.27 (d, 2H,  $J = 8.4$  Hz), 2.35 – 2.31 (m, 4H), 1.13 – 0.97 (m, 12H), 0.73 (t, 6H,  $J = 7.2$  Hz), 0.64 – 0.57 (m, 4H).

**9,9-Dihexyl-9H-fluorene-2,7-diamine (6).**<sup>1, 2</sup> **5** (0.60 g, 1.4 mmol) was added to a 50 mL Schlenk tube equipped with a stir bar. Three purge-pump-thaw cycles were completed before anhydrous ethyl alcohol (10 mL) was added using a syringe. The mixture was stirred, and then 10 % palladium on carbon (59 mg) was added, followed by hydrazine monohydrate (0.66 mL, 13.6 mmol). The mixture was heated using an oil bath at 75 °C for 2 h, after which it was allowed to cool. The contents of the tube were poured into cold distilled water (50 mL), transferred into a separatory funnel and extracted with ethyl acetate (3 x 25 mL). The organic fraction was washed with distilled water (1 x 50 mL) and a saturated aqueous NaCl solution (1 x 50 mL). It was then dried with anhydrous MgSO<sub>4</sub>, filtered, and the solvent was then removed by bubbling N<sub>2</sub> into the mixture. The resulting dark brown oil was reacted with **7** without further purification and characterization.

**9,9-Dioctyl-9H-fluorene-2,7-dicarbaldehyde (8).**<sup>3</sup> 2,7-Dibromo-9,9-dioctyl-9H-fluorene (0.62 g, 1.1 mmol) was dissolved in anhydrous ether (8.5 mL) under N<sub>2</sub> atmosphere in a 25 mL Schlenk tube. *N,N,N',N'*-Tetramethylethylenediamine (0.67 mL, 4.5 mmol) was added before cooling the mixture to -78 °C. A 2.5 M solution of *n*-butyl lithium in hexanes (1.8 mL, 4.5 mmol) was slowly added, and the mixture stirred at -78 °C for 1.5 h, followed by the addition of anhydrous *N,N*-dimethylformamide (1.3 mL, 17 mmol). The mixture was stirred in the cold bath and gradually warmed to room temperature overnight. An aqueous 1.2 N solution of hydrochloric acid (15 mL) was added to the reaction mixture at 0 °C and it was allowed to stir for 25 min. The contents of the tube were then transferred into a separatory funnel and extracted with dichloromethane (3 x

25 mL). The organic fraction was dried with anhydrous Na<sub>2</sub>SO<sub>4</sub>, filtered, and the solvent was removed in vacuo. The resulting oil was purified by silica gel chromatography. The title compound was obtained as an oily, pale yellow solid (404 mg, 80%). <sup>1</sup>H-NMR (acetone-*d*<sub>6</sub>): δ = 10.14 (s, 2H), 8.16 (d, 2H, *J* = 8.0 Hz), 8.08 (s, 2H), 8.00 (dd, 2H, *J* = 8.0 Hz, 1.6 Hz), 2.23 – 2.19 (m, 4H), 1.21 – 1.03 (m, 24H), 0.77 (t, 6H, *J* = 7.0 Hz), 0.63 – 0.55 (m, 4H).

**Copolymer (3).** **8** (0.40 g, 0.90 mmol) and **6** (0.36 g, 0.99 mmol) were dissolved in chloroform (2.0 mL) in a 10 mL pressure tube equipped with a stir bar. Trifluoroacetic acid (7 μL) was added and the solution was heated in an oil bath at 100 °C for four days. The contents of the tube were allowed to cool, after which they were dissolved in a minimum amount of dichloromethane and then precipitated in methanol to produce a dark yellow solid. The precipitate was filtered, washed with cold methanol, hexanes and then ethyl acetate. It was then solubilised in a minimum amount of THF as it was unstable when allowed to dry. The molecular weight of the precipitated polymer was measured by GPC relative to polystyrene standards.  $M_n = 7\,200$  g/mol; PDI = 1.89;  $DP_n = 9$ .

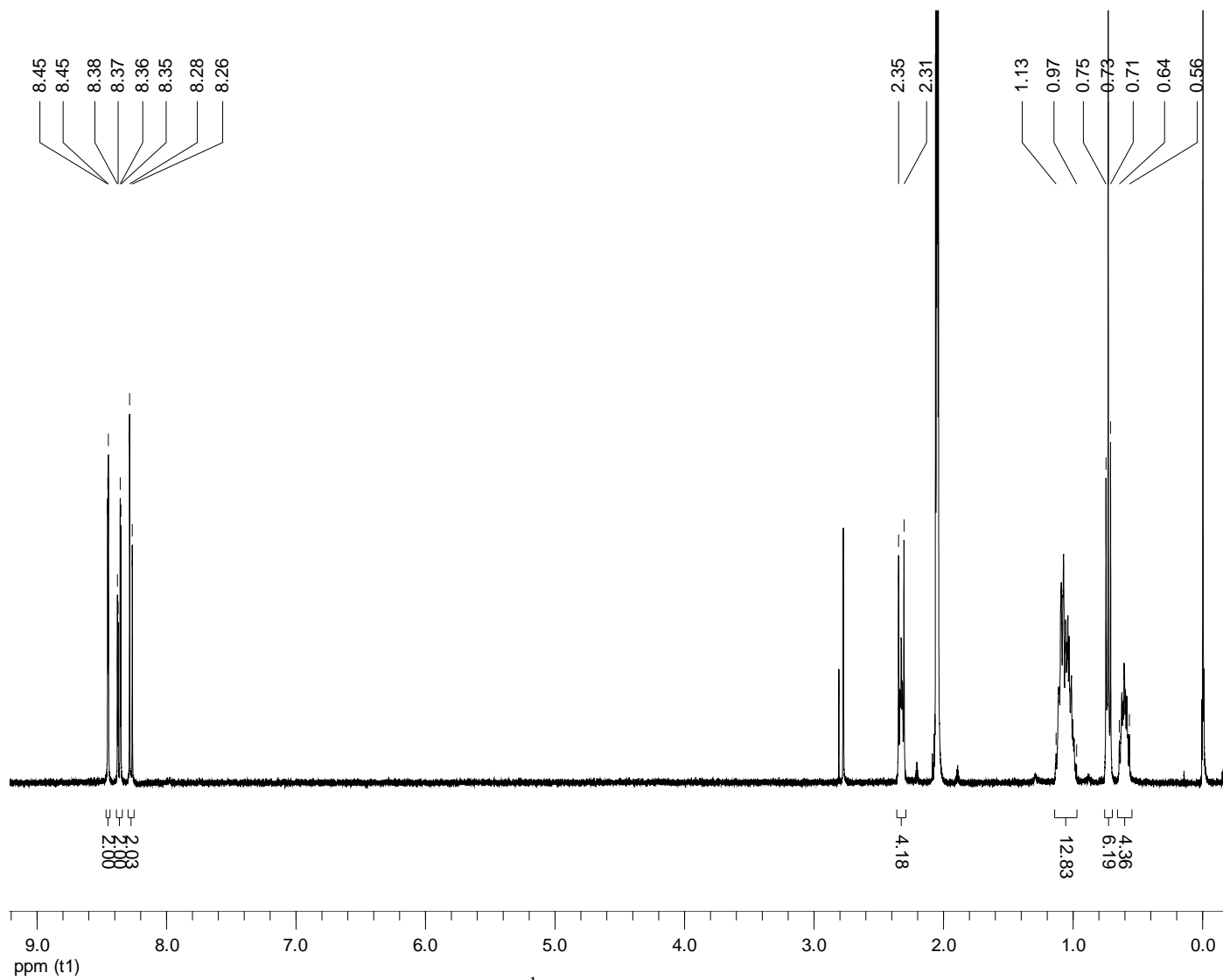


Figure S67.  $^1\text{H}$  NMR of **5** in acetone- $\text{d}_6$ .

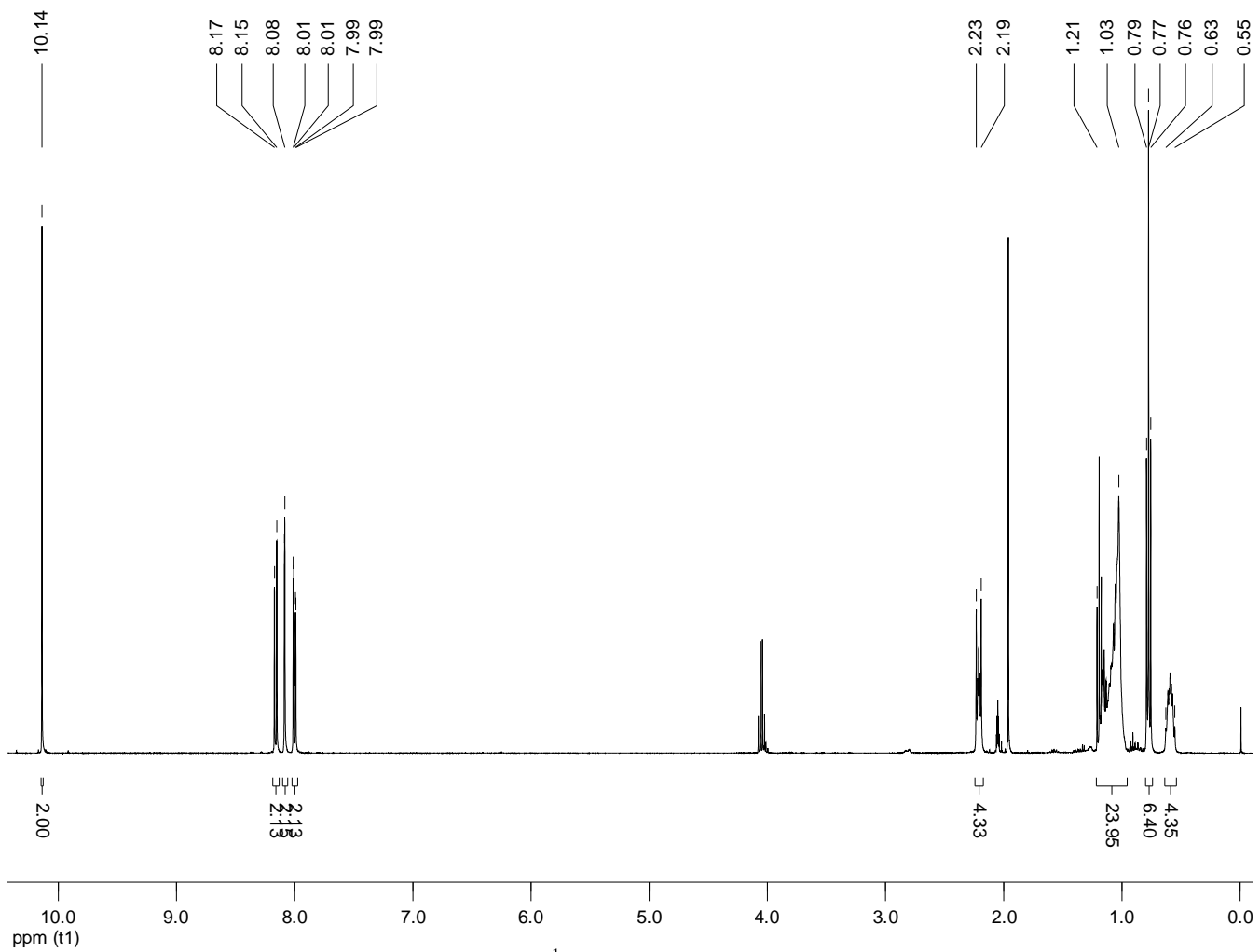


Figure S68.  $^1\text{H}$  NMR **8** in acetone- $\text{d}_6$ .

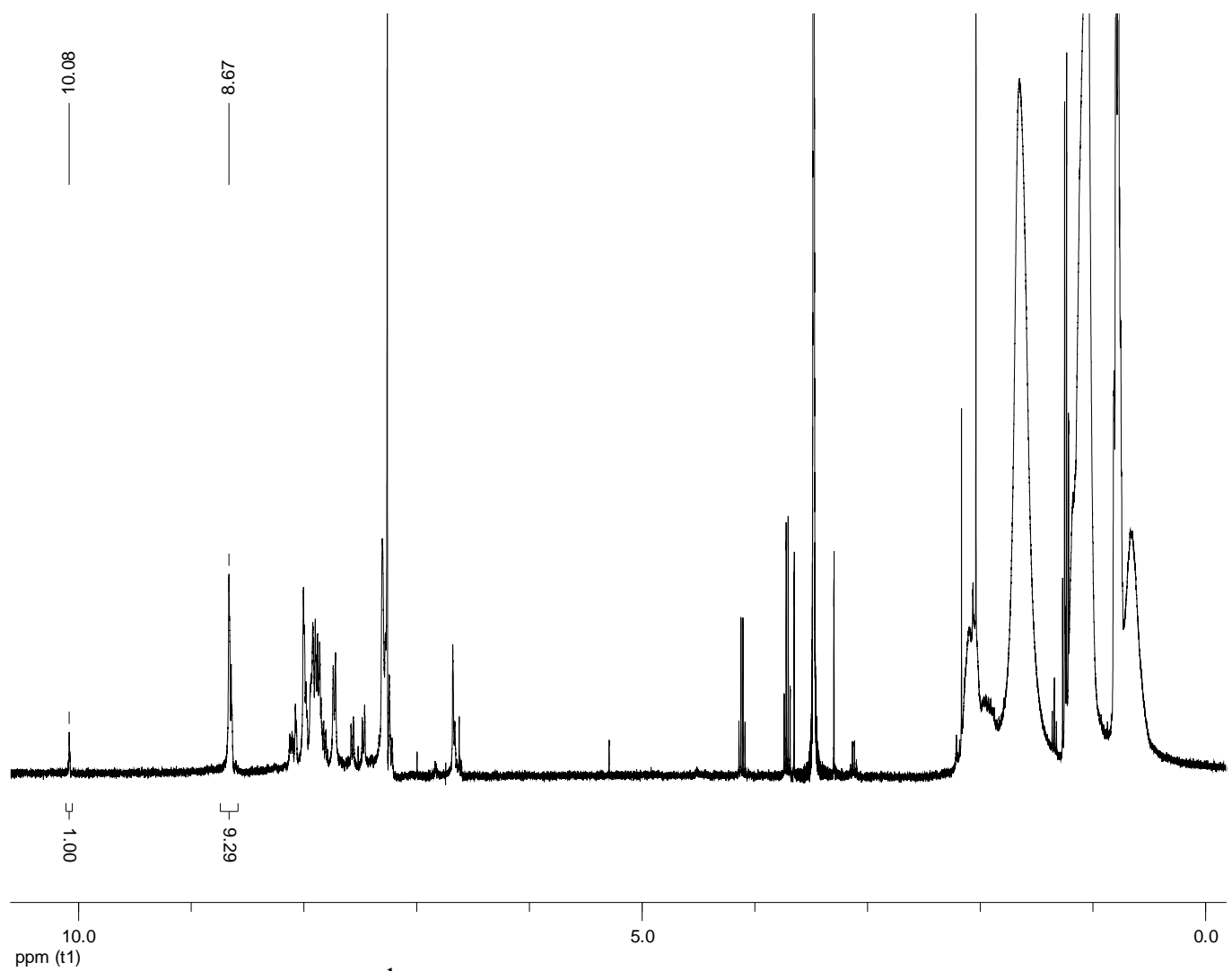
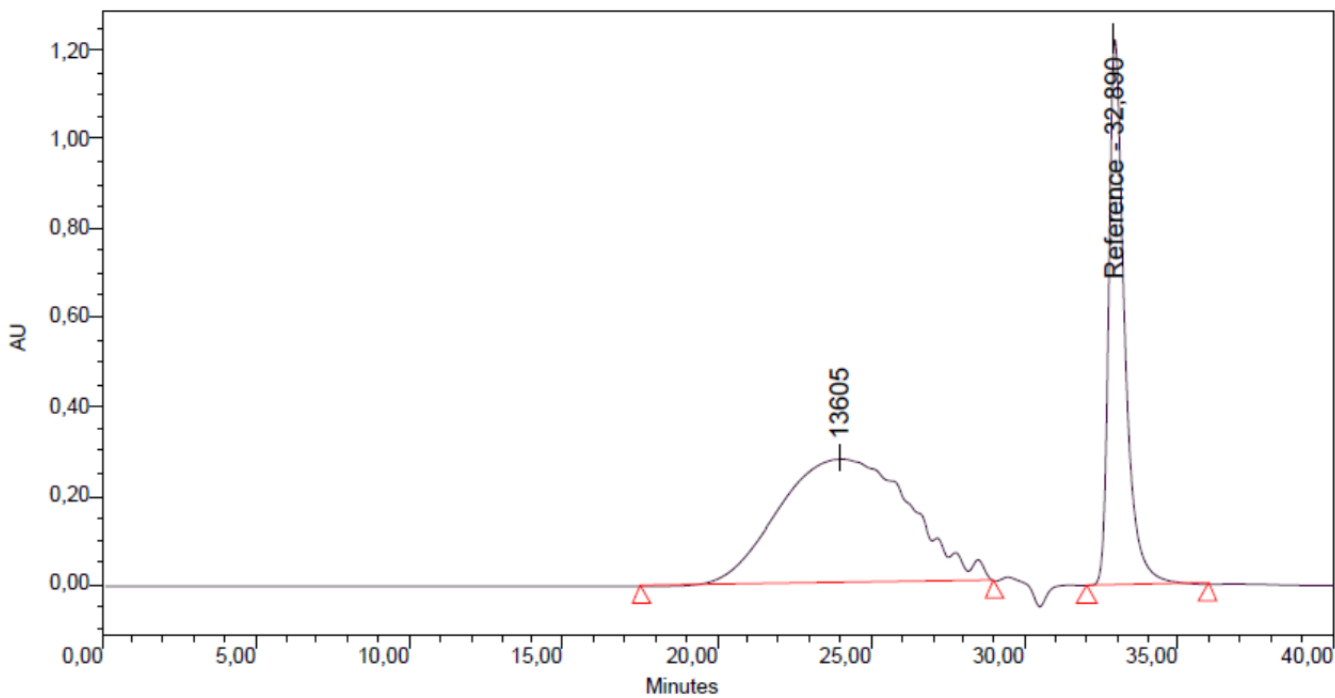


Figure S69.  $^1\text{H}$  NMR of **3** in  $\text{CDCl}_3$  after 84 h of polymerization.



GPC Results

	Dist Name	Elution Volume (ml)	Retention Time (min)	Adjusted RT (min)	Mn	Mw	MP	Mz	Mz+1
1		23,915	23,964	23,915	7214	18421	13605	37730	61473
2		32,822	32,890	32,822					

Figure S70. GPC elugram of **3** in THF relative to polystyrene standards.

## References

1. J. K. Sørensen, J. Fock, A. H. Pedersen, A. B. Petersen, K. Jennum, K. Bechgaard, K. Kilså, V. Geskin, J. r. m. Cornil, T. Bjørnholm and M. B. Nielsen, *J. Org. Chem.*, 2010, **76**, 245-263.
2. S. P. Dudek, M. Pouderoijen, R. Abbel, A. P. H. J. Schenning and E. W. Meijer, *J. Am. Chem. Soc.*, 2005, **127**, 11763-11768.
3. J. J. Intemann, J. F. Mike, M. Cai, S. Bose, T. Xiao, T. C. Mauldin, R. A. Roggers, J. Shinar, R. Shinar and M. Jeffries-El, *Macromolecules*, 2010, **44**, 248-255.